On the highly ordered graphene structure of Non-Graphitic Carbons (NGCs) – a Wide-Angle Neutron Scattering (WANS) study

Supporting information

Authors

Oliver Osswald[1*], Marc O Loeh[2], Felix M Badaczewski[2], Torben Pfaff[3], Henry E Fischer[4], Alexandra Franz[5], Jens-Uwe Hoffmann[5], Manfred Reehuis[5], Peter J Klar[6] and Bernd M Smarsly[1*]

1   Institute of Physical Chemistry, Justus-Liebig-University Giessen, Heinrich-Buff-Ring 17, Giessen, 35392, Germany
2   Schunk Kohlenstofftechnik GmbH, Rodheimer Strasse 59, 35452 Heuchelheim, Germany
3   Lang GmbH & Co. KG, Dillstraße 4, 35625 Hüttenberg, Germany
4   Institut Laue-Langevin, 71 avenue des Martyrs, CS 20156, 38042 Grenoble cedex 9, France
5   Helmholtz-Zentrum Berlin für Materialien und Energie, Hahn-Meitner-Platz 1, 14109 Berlin, Germany
6   Institute of Experimental Physics I, Justus-Liebig-University Giessen, Heinrich-Buff-Ring 16, Giessen, 35392, Germany

*   Correspondence: carbon@oss-wald.de; bernd.smarsly@pyhs.chemie.uni-giessen.de

Supporting information

S1. Data treatment and background correction

S1.1. Refinement by Ruland and Smarsly's algorithm

In principle, the theoretical scattering intensity of the material ($I_{e.u.}$) is a superposition of the coherent scattering (I_{coh}) and the incoherent scattering (I_{incoh}), where the coherent scattering can be calculated by the interlayer and intralayer scattering intensity (I_{inter} and I_{intra}, respectively) and the atomic form-factor of carbon (f_c):

$$I_{e.u.} = I_{coh} + I_{incoh} \tag{1}$$

$$I_{coh, c} = f_c^2 \cdot (I_{inter} + I_{intra}) \tag{2}$$

Beside these structural influences, the calculated theoretical intensity without any experimental influences (I_{calc}) can be calculated by:

$$I_{calc} = k \cdot A \cdot P \cdot I_{e.u.} \tag{3}$$

Hence, k is a normalization constant, which is needed through the different intensities of the incoming radiation and the amount of irradiated material, A is the absorption parameter and P describes the polarization. The Lorentz factor is already considered in the calculation of the coherent scattering intensity and therefore, this parameter does not have to and must not be considered further. Additional information of these correction parameters can be found the work of Osswald and Smarsly [1].

However, a factor considering a fixed irradiated length instead a fixed divergence slit (*AutoColl*), an exponential damping factor (*gFact*) for taking the possibility of a small angle scattering contribution at low scattering vector values as well as two constants (*const$_1$*, *const$_2$*) for considering a linear and a non-linear background, can be used to obtain the full observed intensity (I_{obs}):

$$I_{obs} = 10^\wedge[\log_{10}((1/AutoColl) \cdot gFact \cdot k \cdot A \cdot P \cdot (I_{coh} + I_{incoh})) + const_1) + const_2] \tag{4}$$

Since the parameters *AutoColl*, A, P, I_{coh} and I_{incoh} are clearly and unique to calculate and use, in this study, the parameters k, *gFact*, *const$_1$* and *const$_2$* are from more interest. Hence, k is just a normalization constant, which must be used every time due to the different intensity of the incoming radiation and the different amounts and densities of the used samples. The parameter *const$_1$* causes a constant shift of the whole scattering curve, which is caused by cosmical background radiation, incoherent scattering, sample holder or other general influences during the experiment. *const$_2$* describes a non-linear background, which may be caused by the incoherent scattering due to the incoherent cross section of the atoms. Further information about these parameters and their influence is given in the next section.

S1.2. Background correction

The previous described background correction is very simple and cannot cover the entire background in WANS measurements. Instead, the models of Placzek [2] or Fischer et al. [3] should be used, where the background scattering can be calculated by fitted by a cubic polynomial or a Pseudo-Voigt function with the normalization constant k, the proportion of the Lorentzian/Gaussian function η and the half with at full maximum (FWHM) 2ω (equation (5) and (6), respectively):

$$S(s) = I_{\text{Obs}}(s) - (a \cdot s^2 + b) + 1 \tag{5}$$

$$S(s) = I_{\text{Obs}}(s) - k \cdot (\eta \cdot L(s, \omega) + (1 - \eta) \cdot G(s, \omega)) + 1 \tag{6}$$

$$L(s, \omega) = \frac{1}{1 + \left(\frac{s}{\omega}\right)^2} \tag{7}$$

$$G(s, \omega) = \exp^{-\ln(2) \cdot \left(\frac{s}{\omega}\right)^2} = 2^{-\left(\frac{s}{\omega}\right)^2} \tag{8}$$

Hence, equation (8) should be used for samples containing only a very small of hydrogen, otherwise equation (8) should be used. In Figure S1, the background correction for PF-R 1000 and PF-R 1500 is shown. Since PF-R 1000 consists of a very high amount of hydrogen and therefore, a Pseudo-Voigt background correction is necessary. On the other hand, PF-R 1500 consists of less hydrogen and therefore, the difference is much smaller and for higher heat-treated samples, a Placzek instead of Pseudo-Voigt correction is sufficient. For a hydrogen amount > 0.3 wt. %, a Pseudo-Voigt function should be used to determine the background (Figure S1). For all other samples, a Placzek correction is sufficient. More detailed information about the background correction can be found in the work of Osswald & Smarsly [1].

Using equation (4), the influences of the different parameters can be determined easily. Now, the measured scattering intensity can be turned into a theoretical calculated intensity, which corresponds to the model of Ruland and Smarsly [4]. Hence, k is just a normalization constant, which must be used every time due to the different intensity of the incoming radiation and the different amounts and densities of the used samples. The parameter $const_1$ causes a constant shift of the whole scattering curve, which is caused by cosmical background radiation, incoherent scattering, sample holder or other general influences during the experiment. For the parameter $const_2$, it must be differentiated into two cases: If $const_1 = 0$, then $const_2$ is nothing else than the normalization constant with $const_2 = -\log(k)$.

Additionally, also the parameter $gFact = \exp(g\,s)$ is not that easily to understand. In principle, this parameter should describe a possible influence of a small-angle scattering intensity on the WAXS or WANS data [5]. However, this intensity falls with Porod's law ($I \sim P/s^4$) and the influence of the fluctuation of the graphene sheets in the stacking structure ($I \sim B_{\text{fl}}/s^2$) and overall, the damping of can

be described as a superposition of them as described in the works of Porod, Ruland, Smarsly and coworkers [6–8]. Since, both influences are only small in bulk materials, it can be described by the factor *gFact* well as already done in the references [9–11]. Additionally, the theoretical calculated scattering intensity assumes a hexagonal layer structure, which might not be the case for very disordered structures. Also, resin as precursor results in a porous structure [9,12], which can also interpretated as a degree of disorder in the stacking structure. These different types of additionally disorders causes some damping of the intensity, where the damping is higher at higher values of *s*.

To proof these assumptions, data refinements using *gFact* and *const$_2$* and refinements fixing them to 0 were performed. Overall, there is a significant difference in the refinements for the samples PF-R 1000/1200/1500/1800/2100 and MP 1200/1500, respectively, for all other samples, the values are generally nearly identical. Additionally, the resulting refinements for the refinements $g = 0$/*const$_2$* = fitted and $g = 0$/*const$_2$* $= 0$ are also very similar, only for $g \neq 0$, there is a significant difference (Figure S2). This behavior is directly related to the amount of hydrogen of the sample (Figure 12, Table S2). It seems, that the amount of hydrogen has a direct or indirect influence on the resulting microstructure parameters, even if this incoherent background scattering was subtracted.

However, this differences in the ways of determining the background can be balanced by the additional normalization parameters *const$_2$* and *g*. In the resulting refinements, both parameters are only small and therefore, they can be seen as "smoothing parameters". Therefore, the parameters *const$_2$* and *g* are needed for samples containing hydrogen, since these influences the refinement result directly through the incoherent background indirectly through a higher degree of disorder, which can be described through the additional normalization parameters. These theoretical considerations can also be proofed looking at the refinements. In Figure S2, the refinements for PF-R 1200 and PF-R 3000 are shown. Since PF-R 1000 consists of high amount of hydrogen, the different refinements are slightly different, but overall, *const$_2$* and *g* must be used to get the best result as possible. In contrast, PF-R 3000 is much more ordered and does not consist of any hydrogen and therefore, the refinements are nearly identical. It does not matter, whether *const$_2$* and *g* was used or not and both parameters do not have an influence on the resulting microstructure parameters. Therefore, they can also be used for these samples, since they will be fitted near to 0 in this case.

To conclude this discussion about the background correction and the usage of the normalization constants, the following two points should be considered:

1. For a hydrogen amount > 0.2 %, a Pseudo-Voigt function should be used to determine the background. For all other samples, a Placzek correction is sufficient.

2. The parameters *g* and *const$_2$* should be refined for every sample, since it leads to more exact results for less ordered samples it does not influence higher ordered samples.
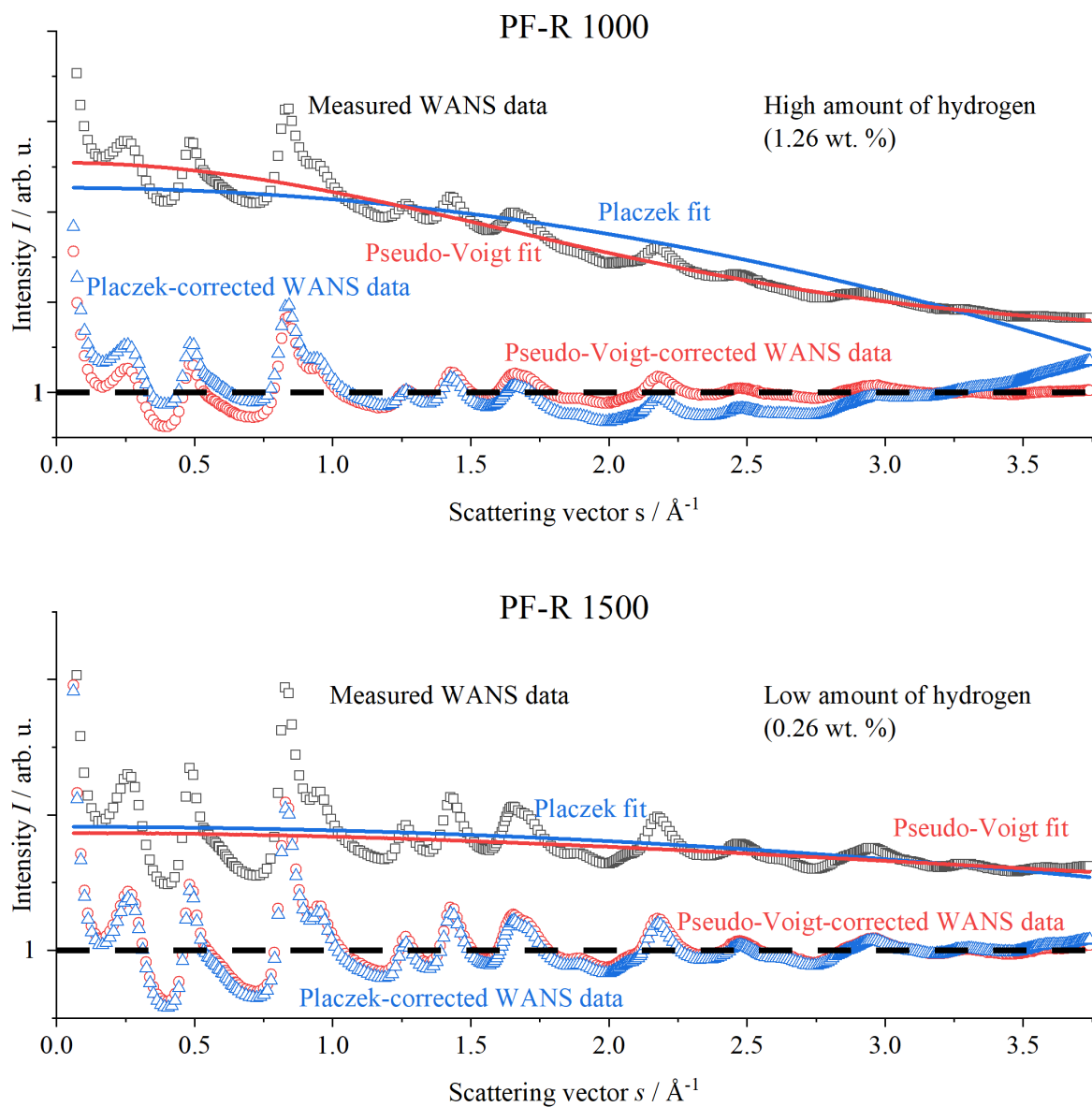
Figure S1 Background correction using a Pseudo-Voigt function (red) for PF-R 1000, which contains a significant amount of hydrogen in contrast du a Placzek correction (blue), which is used for samples consist of only a few hydrogen (< 0.2 %). For PF-R 1500, the difference is only small and therefore, the Placzek correction is sufficient for temperatures with less hydrogen (= higher heat-treatment temperatures). Only every 3rd measured point is shown.
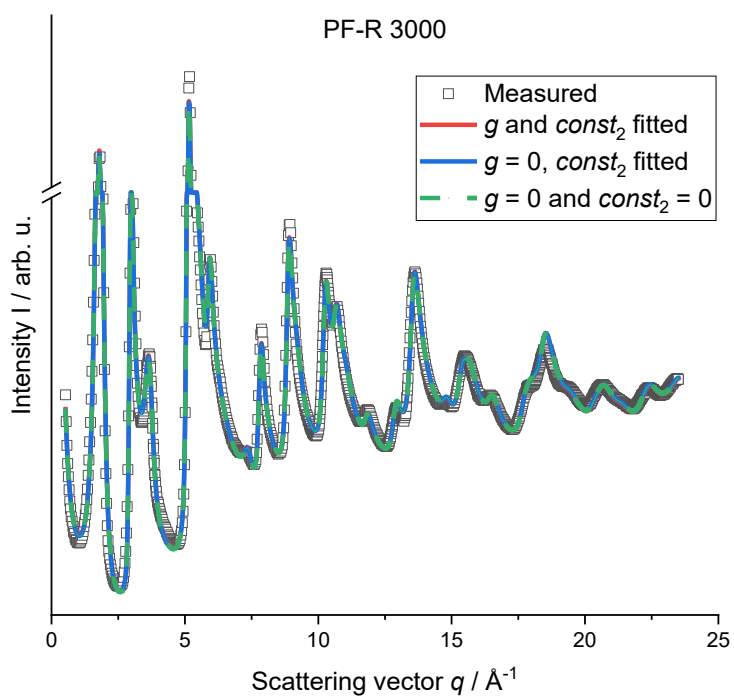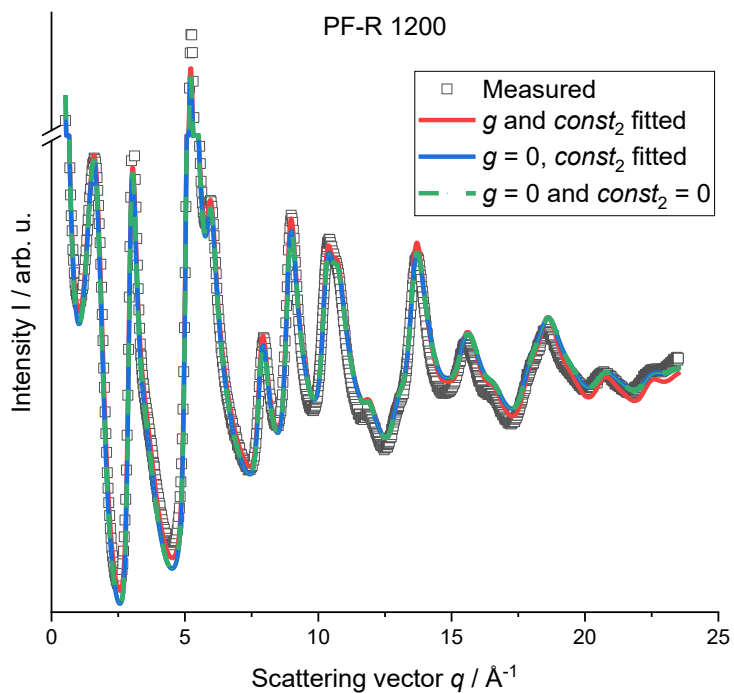
Figure S2 Example refinements for PF-R 1200 and PF-R 3000 using three different types of normalization correction (red: g and $const_2$ fitted, blue: $g = 0$, $const_2$ fitted, green: $g = 0$ and $const_2 = 0$). Overall, the differences are only very small and therefore, it is recommended to use g and $const_2$ during the refinement, since it leads to more comparable and exact results.

S2. Overview about the refined microstructure

S2.1. Results for the phenol-formaldehyde resin (PF-R) temperature series

S2.1.1. WANS-data refinement for the phenol-formaldehyde resin (PF-R) temperature series
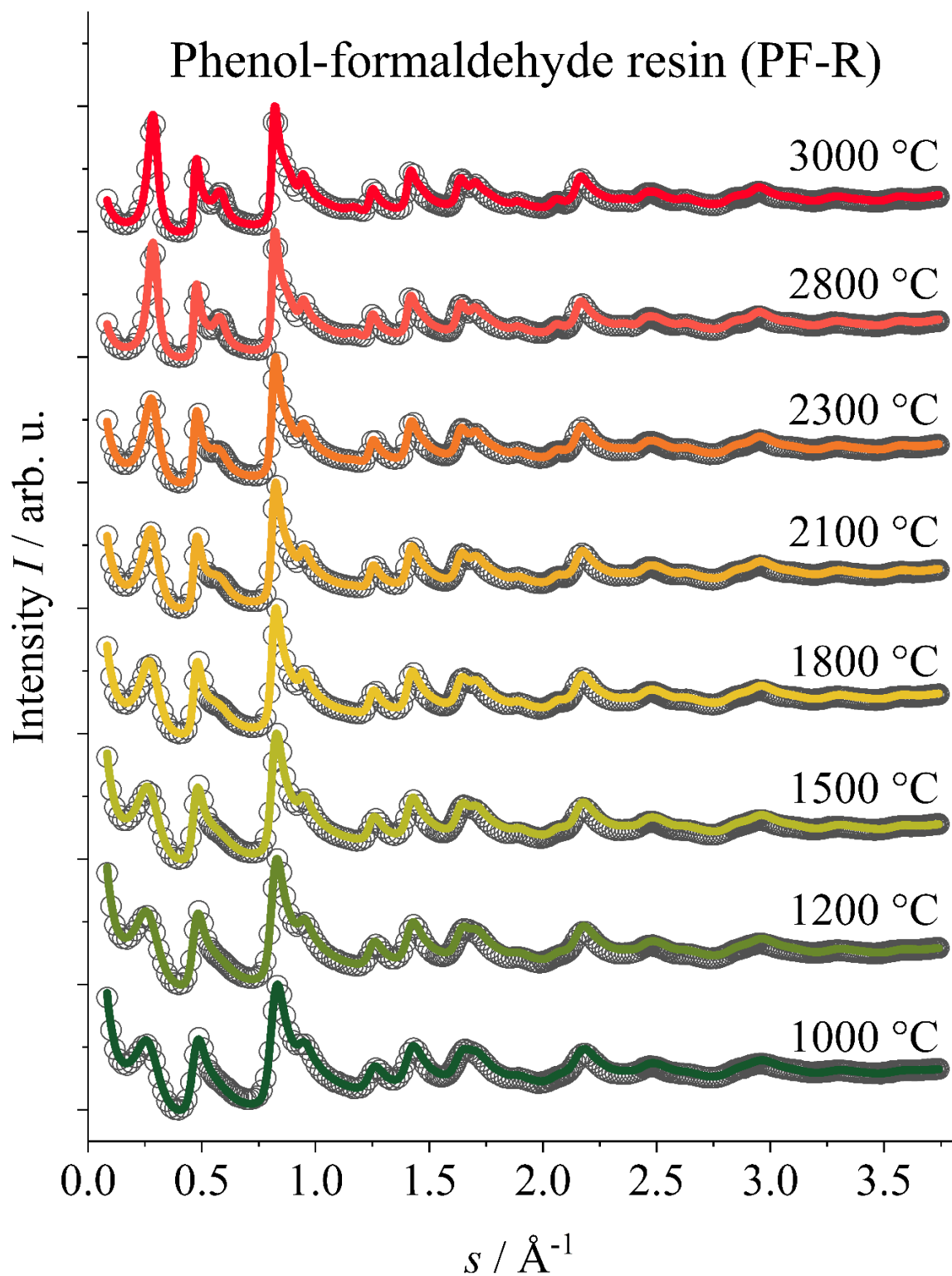
Figure S3   WANS-data refinement for the phenol-formaldehyde resin (PF-R) temperature series.

S2.1.2. Microstructure parameters for the phenol-formaldehyde resin (PF-R) temperature series

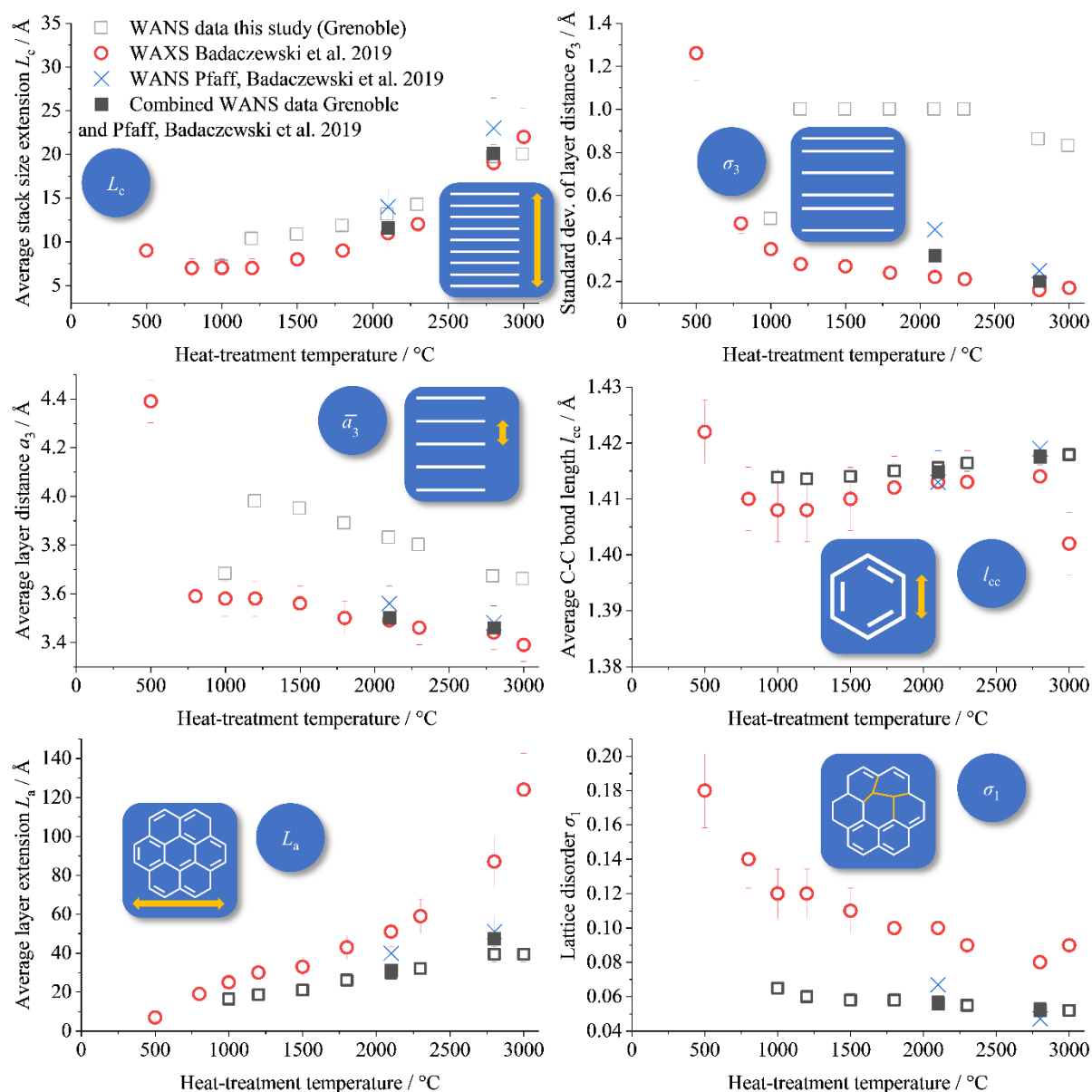**Figure S4**   Refined microstructure data for phenol-formaldehyde resin (PF-R) as precursor (black border-only: this study (WANS Grenoble), red: Badaczewski et al. (WAXS) [1], blue: Pfaff, Badaczewski et al. (WANS Berlin) [2], black filled: combined WANS data from Grenoble and Berlin).

S2.1.3. Stack structure of the phenol-formaldehyde resin (PF-R) temperature series

Regarding to 3.2.1 in the main article, another important point to analyze and determine the disorder of the stacking structure is the parameter κ_c, which describes the polydispersity of the stack height. In the work of Badaczewski et al. [1], these parameter does not have any clear tendency, but they are spread between 0.1 and 1, where 0 means no and 1 a high polydispersity of the stack height. Since this parameter has only a very small influence on the scattering curve, it is nearly impossible to refine this parameter in a meaningful way using wide-angle X-ray scattering at a common copper radiation wavelength ($\lambda = 1.54$ Å). Using neutron scattering at a lower wavelength, higher ordered reflections without any damping from the atomic form factor become visible. Therefore, it is possible to also refine the polydispersity of the stack height. In the case of the phenol-formaldehyde resin, this value decreases from 0.45 at 1000 °C to 0.35 at 3000 °C, which means, the stack height become more unique at higher heat treatment temperatures.

The last parameter describing the order of the stacks is the homogeneity η. This parameter describes, if the sheets are completely parallel and perfectly stacked on each other ($\eta = 1$) or not ($\eta < 1$). The homogeneity is increasing from 0.94 to 1 (perfectly homogeneous), which means an increasing degree of order in the stacking structure. These values are higher than in the reference, where the homogeneity also does not have a clear dependent tendency of the heat treatment, but overall, the order of magnitudes of all parameters are in a good agreement with the WAXS data measured by of Badaczewski et al. [1]. Therefore, also the tendency for the average stack height (L_c) is comparable to the reference, even if the absolute values are a little bit higher. A higher stack height, which means nothing else than a bigger crystallite size, causes higher and sharper reflections in the scattering pattern, while a higher disorder causes smaller and broader reflections, so also bigger stack height balances the high values of σ_3 and the evaluation of the WANS data of this study is comparable and the results consistent with the reference, even if the absolute values are different.

S2.2. Results for the mesophase pitch (MP) temperature series

S2.2.1. WANS-data refinement for the mesophase pitch (MP) temperature series
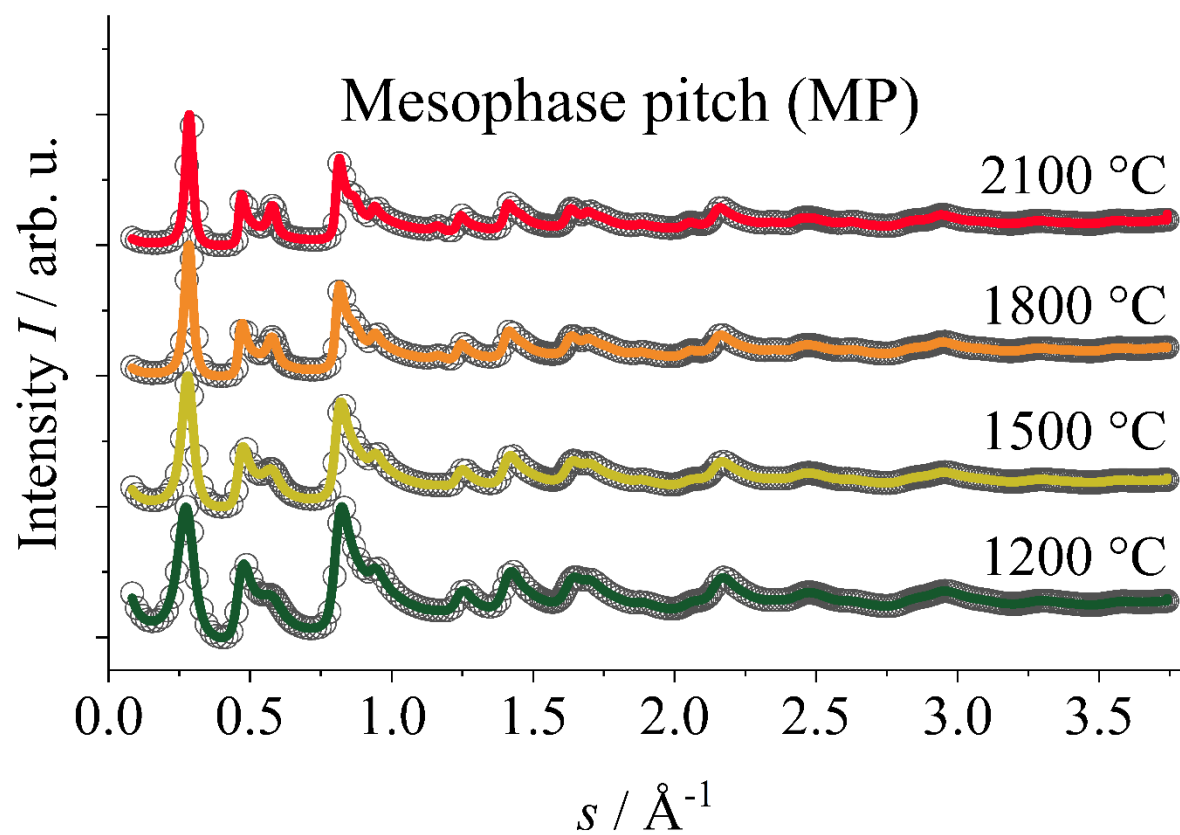
Figure S5   WANS-data refinement for the mesophase pitch (MP) temperature series.

S2.2.2. Microstructure parameters for the mesophase pitch (MP) temperature series

Figure S6   Refined microstructure data for a mesophase pitch (MP) as precursor (black border-only: this study (WANS Grenoble), green: Loeh et al. (WAXS) [3], red: Badaczewski et al. (WAXS) [1], blue: Pfaff, Badaczewski et al. (WANS Berlin) [2], black filled: combined WANS data from Grenoble and Berlin).

S2.3. Results for the low softening-point pitch (LSPP) temperature series

S2.3.1. WANS-data refinement for the low softening-point pitch (LSPP) temperature series
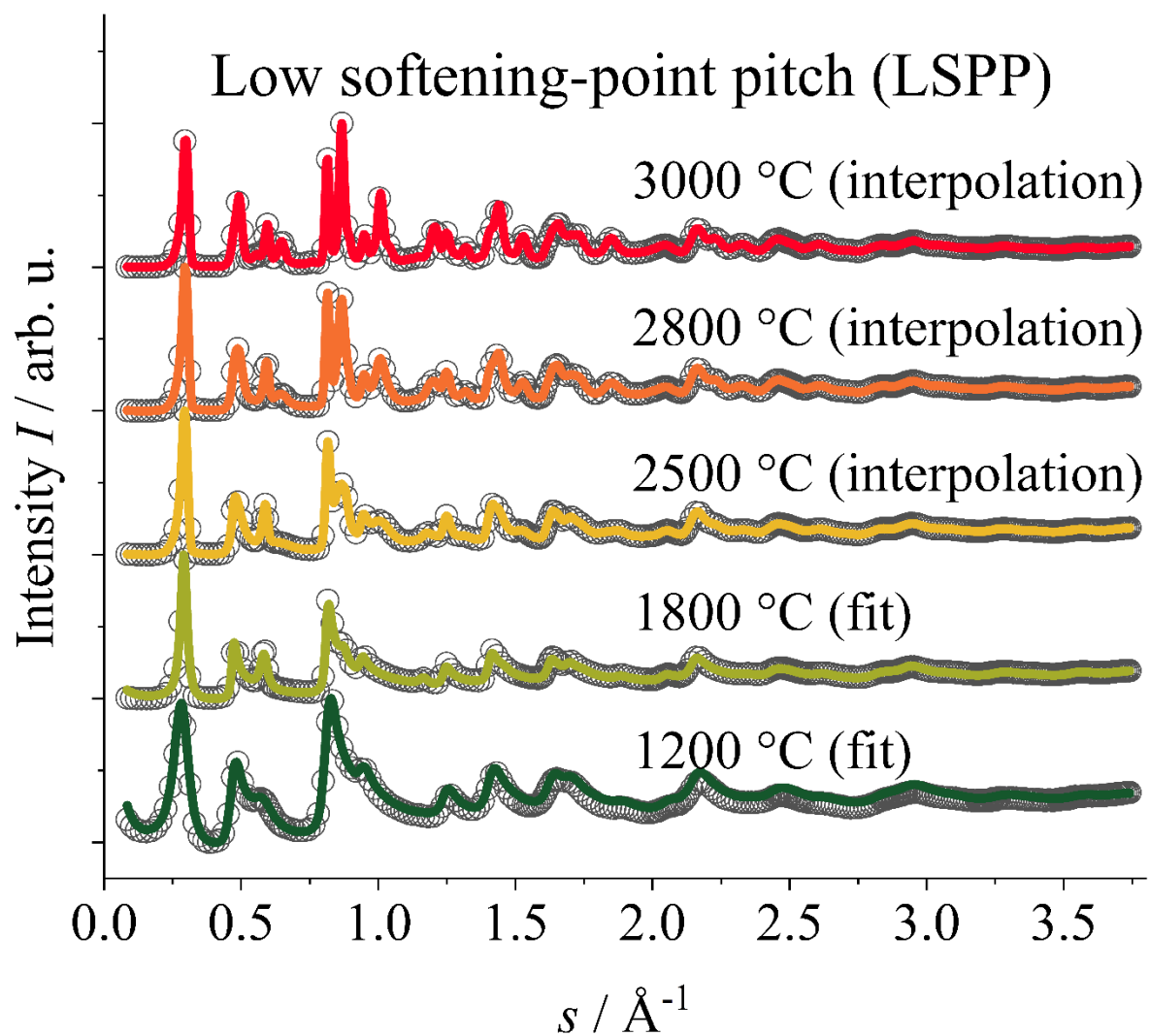
Figure S7 WANS-data refinement (1200 °C and 1800 °C) for the low softening-point pitch (LSPP) temperature series. For 2500 °C, 2800 °C and 3000 °C, the data could not be refined using the model of Ruland & Smarsly [4] due to the "mixed" (*hkl*)-reflections. Therefore, the data was just interpolated.

S2.3.2. Microstructure parameters for the low softening-point pitch (LSPP) temperature series
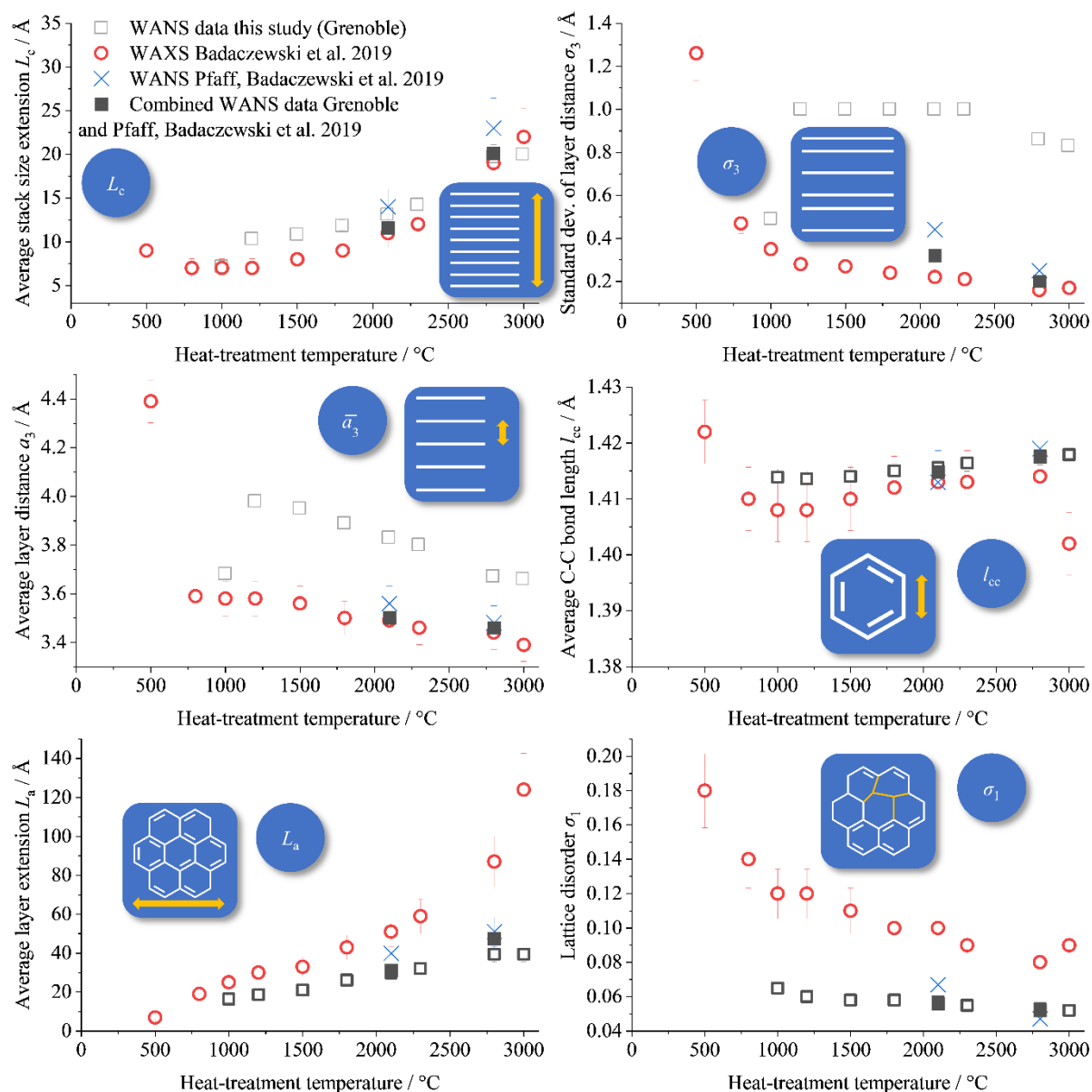

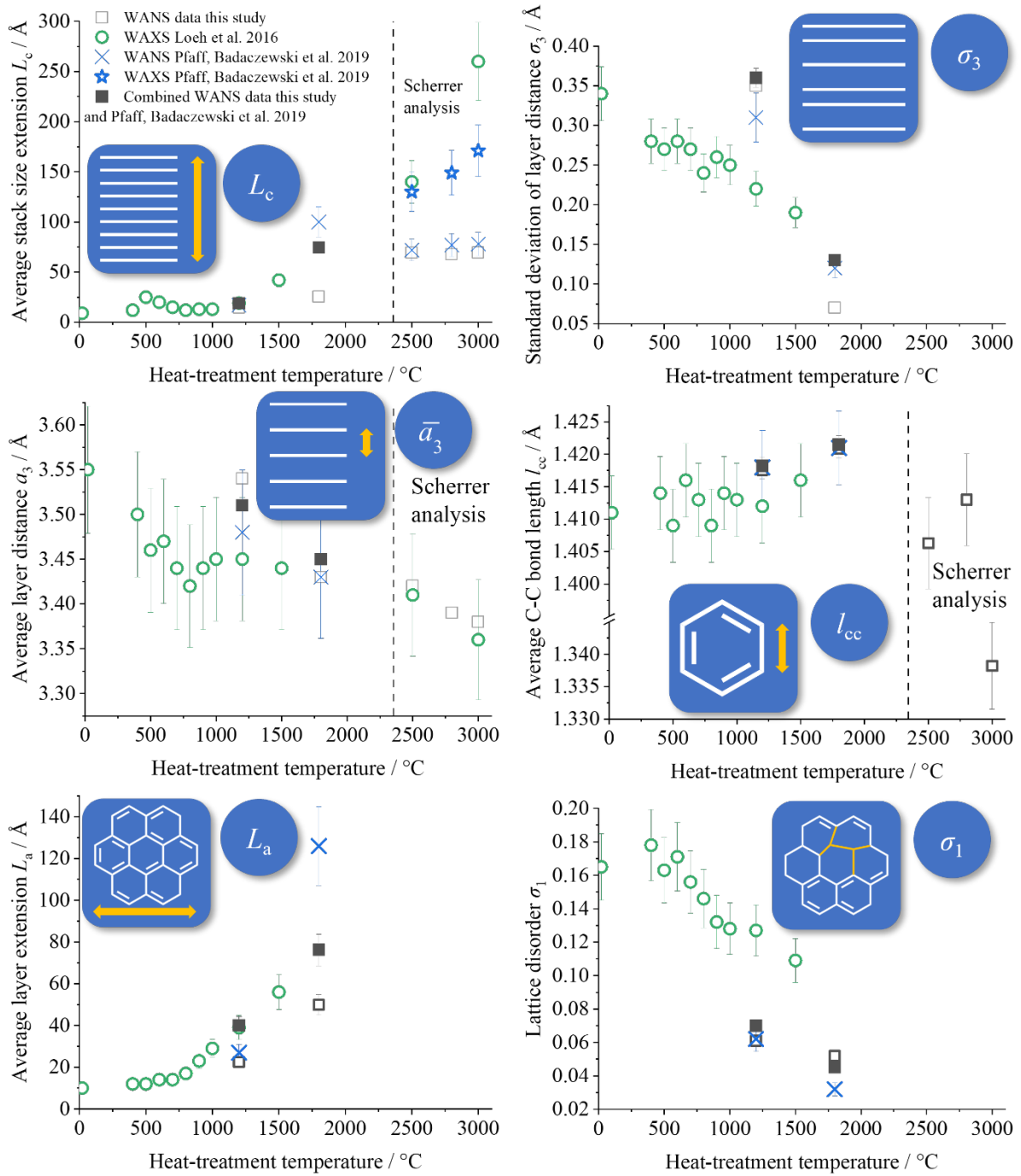**Figure S8** Refined microstructure data for a low softening-point pitch (LSPP) as precursor (black border-only: this study (WANS Grenoble), green: Loeh et al. (WAXS) [3], blue: Pfaff, Badaczewski et al. (WANS Berlin) [2], black filled: combined WANS data from Grenoble and Berlin).

S2.4. Comparison between measured wide-angle neutron scattering data of this study to wide-angle X-ray and neutron (WAXS/WANS) to works of Badaczewski, Loeh, Pfaff et al. [1–3]

△ Grenoble WANS data PF-R
○ Grenoble WANS data MP
□ Grenoble WANS data LSPP
▲ Combined Grenoble/Berlin WANS data PF-R
● Combined Grenoble/Berlin WANS data MP
■ Combined Grenoble/Berlin WANS data LSPP
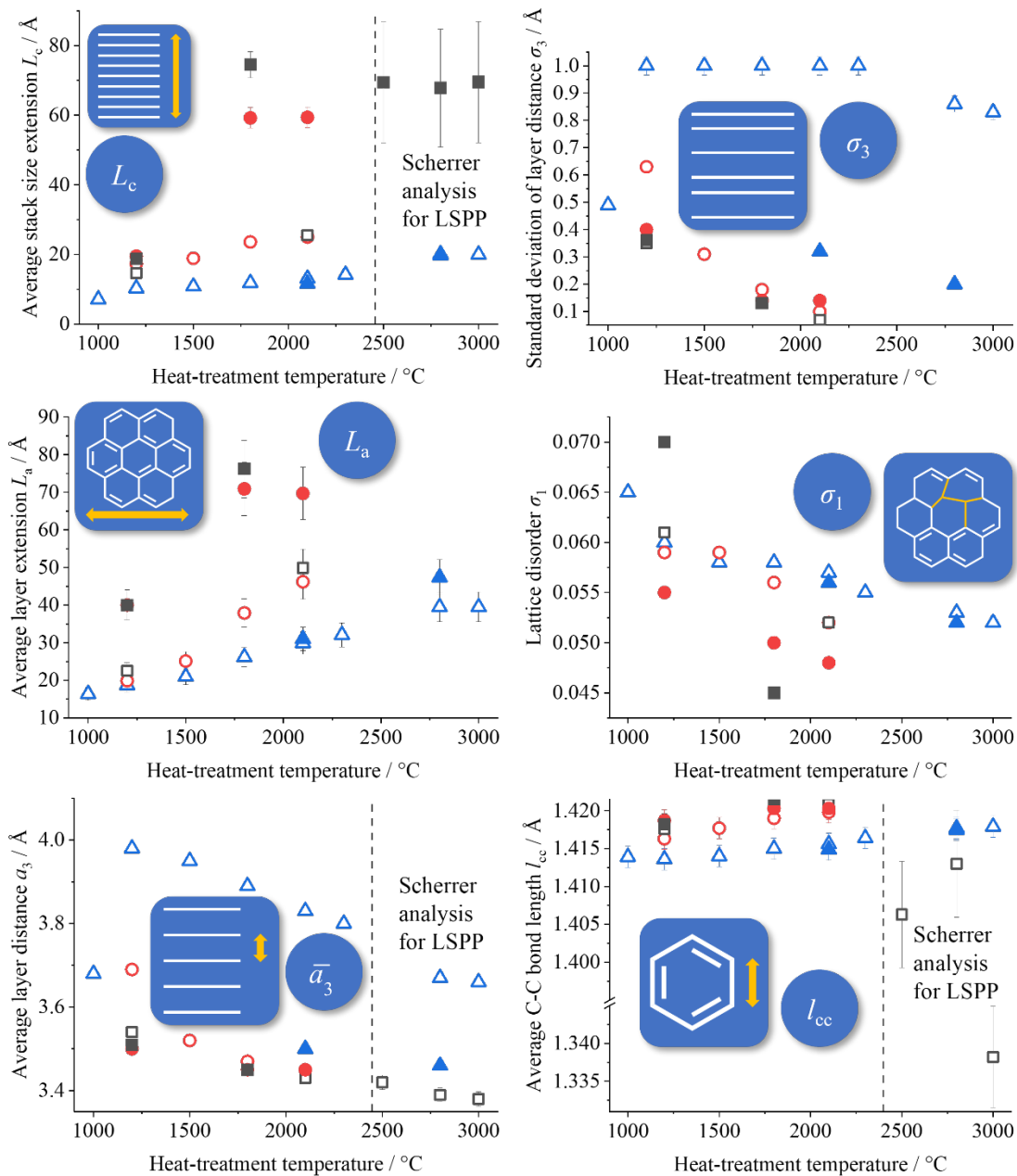
Figure S9 Refined microstructure data comparison between the different precursors (black: phenol-formaldehyde resin (PF-R), red: mesophase pitch (MP), blue: low softening-point pitch (LSPP)). Border-only: Refinement from WANS data from Grenoble (this study); filled: combined WANS data from Grenoble and Berlin (Pfaff, Badaczewski et al. 2019 [2])).

Table S1 Overview about final resulting microstructure parameters. Since phenol-formaldehyde resin (PF-R) is non-graphitizable, the samples still consist of a certain degree of disorder, even hat high heat-treatment temperatures. In contrast, the mesophase pitch (MP) and the low softening-point pitch (LSPP) consist of more ordered aromatic systems in the precursor, so the resulting microstructure is more graphite like at high heat-treatment temperatures. Since the softening-point is lower for LSPP, it is better graphitizable than MP. A detailed description as well as a figure of the meaning of it, can be found in the work of Osswald and Smarsly [5]. The numbers in brackets are the results from the combination of the WANS data from Grenoble and Berlin.

	L_c / Å	N	$\bar{a}_3$ / Å	$a_{3\min}$ / Å	σ_3 / Å	η	L_a / Å	l_{cc} / Å	σ_1
Phenol-formaldehyde resin (PF-R)									
Max. error	5 %	7.5 %	0.1 %	3.3 %	3.3 %	5 %	10 %	0.1 %	2 %
PF-R 1000	7.1	1.9	3.68	3.12	0.49	0.94	16.4	1.4139	0.065
PF-R 1200	10.3	2.6	3.98	3.21	1	0.95	18.7	1.4136	0.060
PF-R 1500	10.8	2.7	3.95	3.24	1	0.96	21.0	1.4140	0.058
PF-R 1800	11.8	3.0	3.89	3.32	1	0.95	26.2	1.4150	0.058
PF-R 2100	13.1 (11.6)	3.4 (3.3)	3.83 (3.5)	3.36 (2.74)	1 (0.32)	0.96 (0.87)	29.9 (31)	1.4156 (1.4149)	0.057 (0.056)
PF-R 2300	14.2	3.7	3.80	3.38	1	0.98	32.1	1.4164	0.055
PF-R 2800	19.7 (20.1)	5.4 (5.8)	3.67 (3.46)	3.39 (3.08)	0.86 (0.20)	1 (0.94)	39.5 (47.4)	1.4177 (1.4175)	0.053 (0.052)
PF-R 3000	20	5.5	3.66	3.39	0.83	1.00	39.5	1.4179	0.052

Mesophase pitch (MP)

	L_c / Å	N	$\overline{a}_3$ / Å	$a_{3\text{min}}$ / Å	σ_3 / Å	η	L_a / Å	l_{cc} / Å	σ_1
Max. error	5 %	7.5 %	0.1 %	3.3 %	3.3 %	5 %	10 %	0.1 %	2 %
MP 1200	17.3 (19.5)	4.7 (5.6)	3.69 (3.5)	3.28 (3.3)	0.63 (0.40)	1 (1)	19.9 (40)	1.4163 (1.4187)	0.059 (0.055)
MP 1500	18.9	5.4	3.52	3.27	0.31	1	25.1	1.4177	0.059
MP 1800	23.6 (59.2)	6.8 (17.1)	3.47 (3.45)	3.37 (3.33)	0.18 (0.14)	1 (0.99)	37.9 (70.9)	1.4190 (1.4203)	0.056 (0.050)
MP 2100	25.0 (59.4)	7.3 (17.2)	3.45 (3.45)	3.39 (3.34)	0.10 (0.14)	1 (0.99)	46.2 (69.7)	1.4198 (1.4203)	0.052 (0.048)

Low softening-point pitch (LSPP) (2500 °C and higher only evaluated by Scherrer analysis)

	L_c / Å	N	$\overline{a}_3$ / Å	a_{3min} / Å	σ_3 / Å	η	L_a / Å	l_{cc} / Å	σ_1
Max. error	5 %	7.5 %	0.1 %	3.3 %	3.3 %	5 %	10 %	0.1 %	2 %
LSPP 1200	14.6 (18.7)	4.1 (5.3)	3.54 (3.51)	3.21 (3.11)	0.35 (0.36)	1.00 (1.00)	22.5 (40.0)	1.4176 (1.4182)	0.061 (0.07)
LSPP 1800	25.5 (74.5)	7.4 (21.6)	3.43 (3.45)	2.76 (3.36)	0.07 (0.13)	1.00 (0.99)	49.9 (76.2)	1.4209 (1.4215)	0.052 (0.045)

Scherrer analysis (higher error bars)

	L_c / Å	N	$\overline{a}_3$ / Å	a_{3min} / Å	σ_3 / Å	η	L_a / Å	l_{cc} / Å	σ_1
LSPP 2500	69.4 (72)		20.3	3.42				1.4063	
LSPP 2800	67.8 (77)		20.0	3.39				1.4130	
LSPP 3000	69.5 (78)		20.6	3.38				1.3382	

S3. Combination of WANS-data

For 7 samples, WANS data from two different experiments were measured and can be combined (PF-R 2100/2800, MP 1200/1800/2100, LSPP 1200/1800). The advantages of the combination have already been discussed in the main article, so only the practical implementation is shown here (Figures S10 and S11).

In principle, the raw data (part A) from Berlin was adjusted to fit the raw data from Grenoble using a linear function (only stretching and moving) in the range from $1.4\ \text{Å}^{-1} < s < 1.5\ \text{Å}^{-1}$. Afterwards, the already known background correction determined from the WANS data from Grenoble was used to correct both, the WANS data from Grenoble and from Berlin. For the combined data, for $s < 1.45\ \text{Å}^{-1}$, the part from Berlin, and for $s > 1.45\ \text{Å}^{-1}$ the part from Grenoble was used.
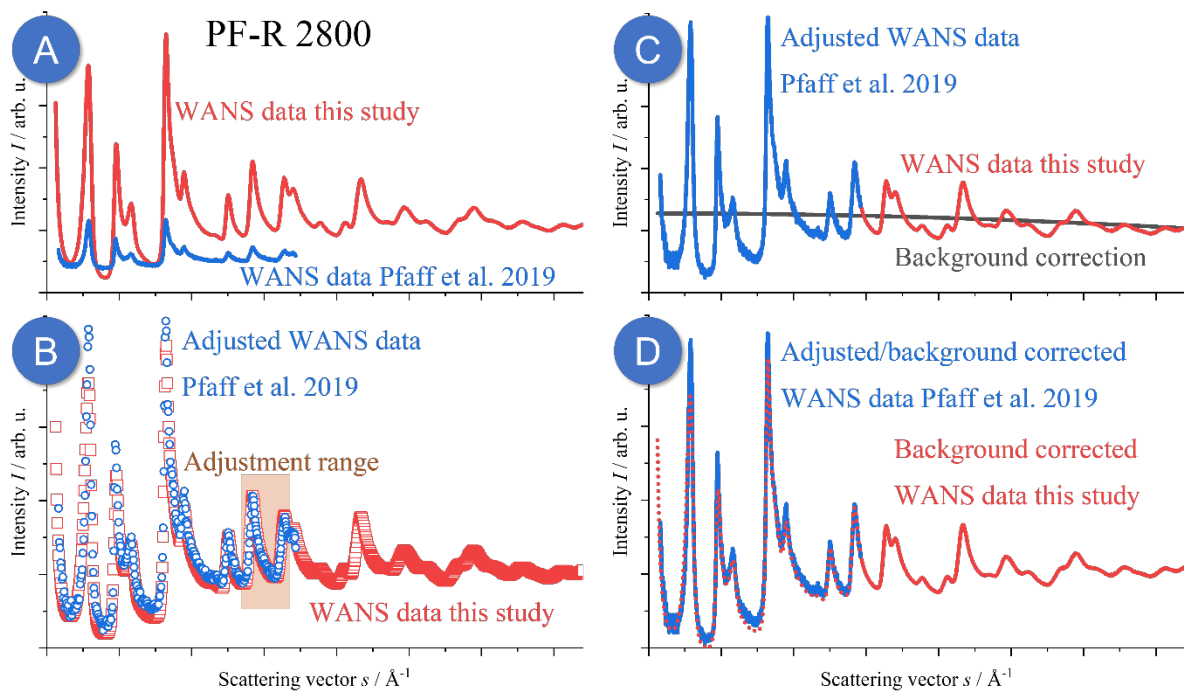
Figure S10 Combination of WANS data for the phenol-formaldehyde heat-treated at 2800 °C measured for this study in Grenoble and already measured by Pfaff, Badaczewski et al. in Berlin [2].
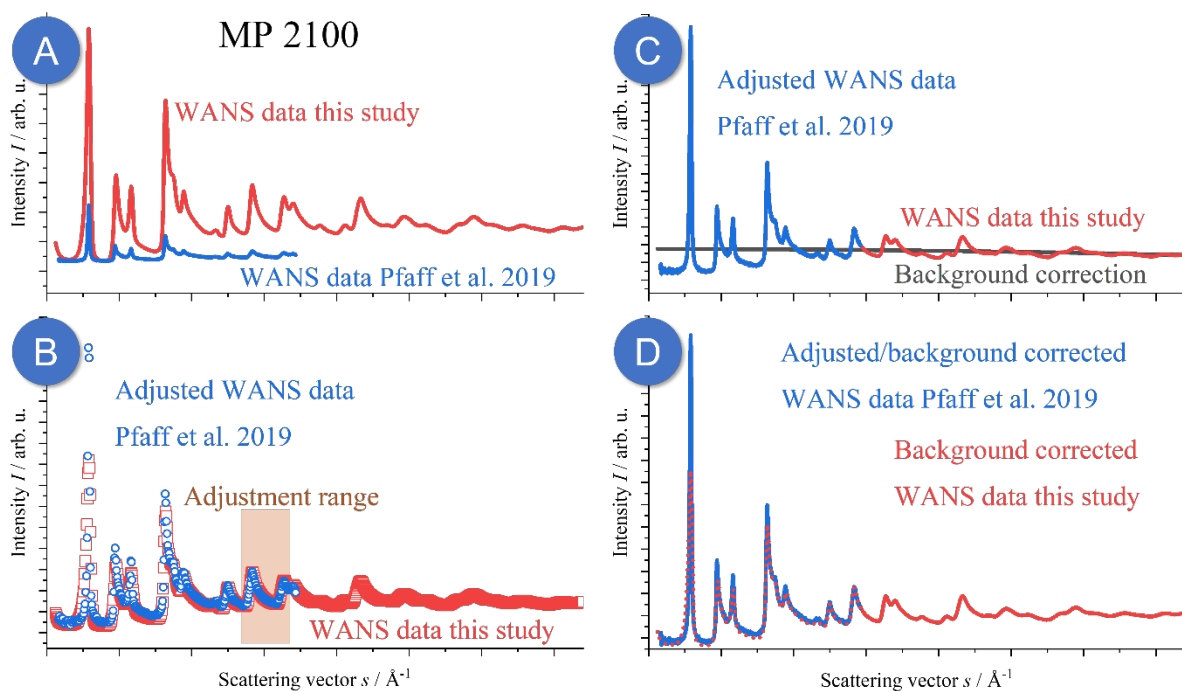
Figure S11 Combination of WANS data for the mesophase pitch heat-treated at 2100 °C measured for this study in Grenoble and already measured by Pfaff, Badaczewski et al. in Berlin [2].

S4. Elemental analysis

Table S2   Overview of the elemental analysis of all measured samples. PF-R = phenol-formaldehyde resin, MP = mesophase pitch, LSPP = low softening-point pitch. Sulfur was only measured for the LSPP series.

Precursor	Heat treatment temperature	Carbon (C)	Hydrogen (H)	Nitrogen (N)	Oxygen (O)	Sulfur (S)
PF-R	1000 °C	95.90%	1.26%	0.64%	0.86%	
PF-R	1200 °C	99.20%	0.43%	0.40%	0.16%	
PF-R	1500 °C	99.50%	0.26%	0.18%	0.25%	
PF-R	1800 °C	99.70%	0.16%	0.01%	0.11%	
PF-R	2100 °C	99.80%	0.13%	0.01%	0.08%	
PF-R	2300 °C	99.80%	0.12%	0.01%	0.07%	
PF-R	2800 °C	99.90%	0.05%	0.01%	0.06%	
PF-R	3000 °C	100.00%	0.00%	0.01%	0.05%	
MP	1200 °C	98.70%	0.40%	0.78%	0.15%	
MP	1500 °C	99.40%	0.24%	0.34%	0.07%	
MP	1800 °C	100.00%	0.15%	0.01%	0.04%	
MP	2100 °C	99.80%	0.15%	0.01%	0.04%	
LSPP	1200 °C	96.20%	0.19%	1.01%	0.17%	0.40%
LSPP	1800 °C	97.80%	0.00%	0.96%	0.05%	0.10%
LSPP	2500 °C	97.10%	0.00%	0.92%	0.06%	0.10%
LSPP	2800 °C	97.20%	0.00%	0.85%	0.04%	0.00%
LSPP	3000 °C	97.50%	0.00%	0.81%	0.06%	0.00%
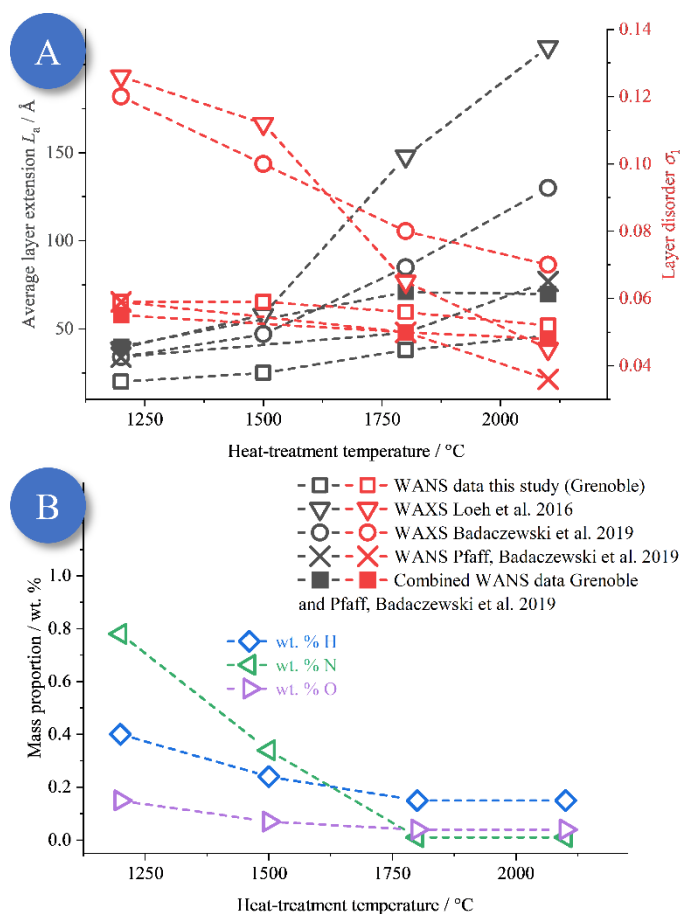
Figure S12 Comparison of the layer extension (L_a) und disorder (σ_1) and stack height (L_c) und disorder (σ_3) to the elemental analysis for a mesophase pitch (MP) as precursor. Since foreign atoms as oxygen and nitrogen cannot build perfect sp^2-hybridizes layers, the presence of it hinders the formation of such layers. Therefore, with a decreasing amount of such atoms leads to bigger and higher ordered layers. The values of L_c and σ_3 are not shown here, because their determination does not possess sufficient accuracy.
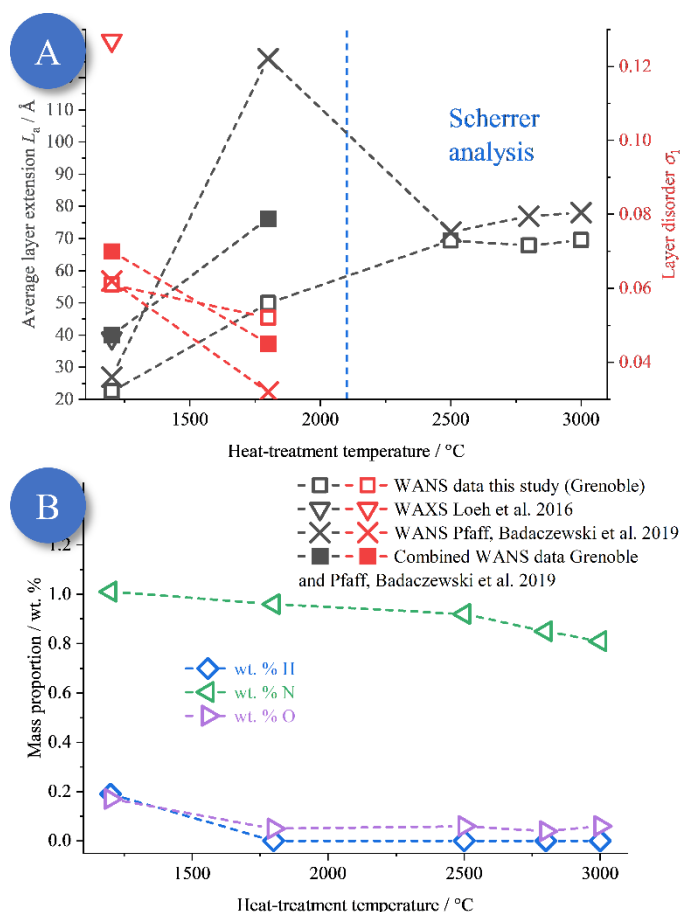
Figure S13 Comparison of the layer extension (L_a) und disorder (σ_1) and stack height (L_c) und disorder (σ_3) to the elemental analysis for the low softening-point pitch (LSPP) as precursor. Since foreign atoms as oxygen and nitrogen cannot build perfect sp^2-hybridizes layers, the presence of it hinders the formation of such layers. Therefore, a decreasing amount of such atoms leads to bigger and higher ordered layers. Additionally, the complete absence of oxygen seems to be a good indicator for the presence of a three-dimensionally ordered graphite-like structure (LSPP 2800/3000). The values of L_c and σ_3 are not shown here, because their determination does not possess sufficient accuracy.

S5. Results, microstructure parameters and comparison to literature
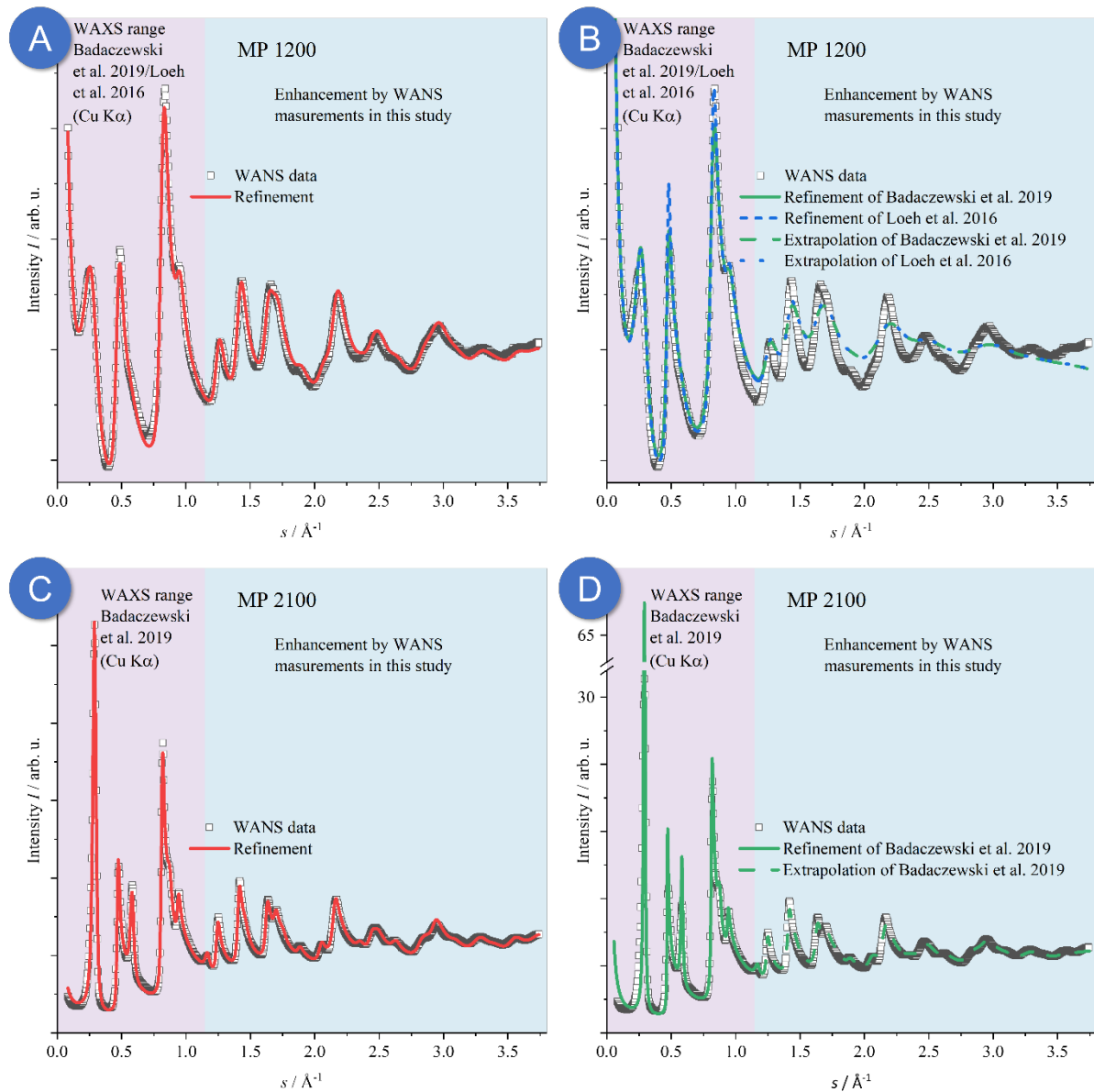
Figure S14 Refinement for MP 1200 and MP 2100 (mesophase pitch heat-treated at 1200 °C/2100 °C). In this figure, only WANS data collected in Grenoble and not the combined WANS data are shown. Red: Refinement of the WANS data. Green/blue: Simulated WANS data using the results from previous WAXS refinements. Especially for MP 2100, the simulated (002)-reflection at $s \sim 0.25$ Å is too small compared to the measured data. The reason is the bad s-space resolution ($\Delta s/s$), which causes a broadening in the WANS data at lower values of s.
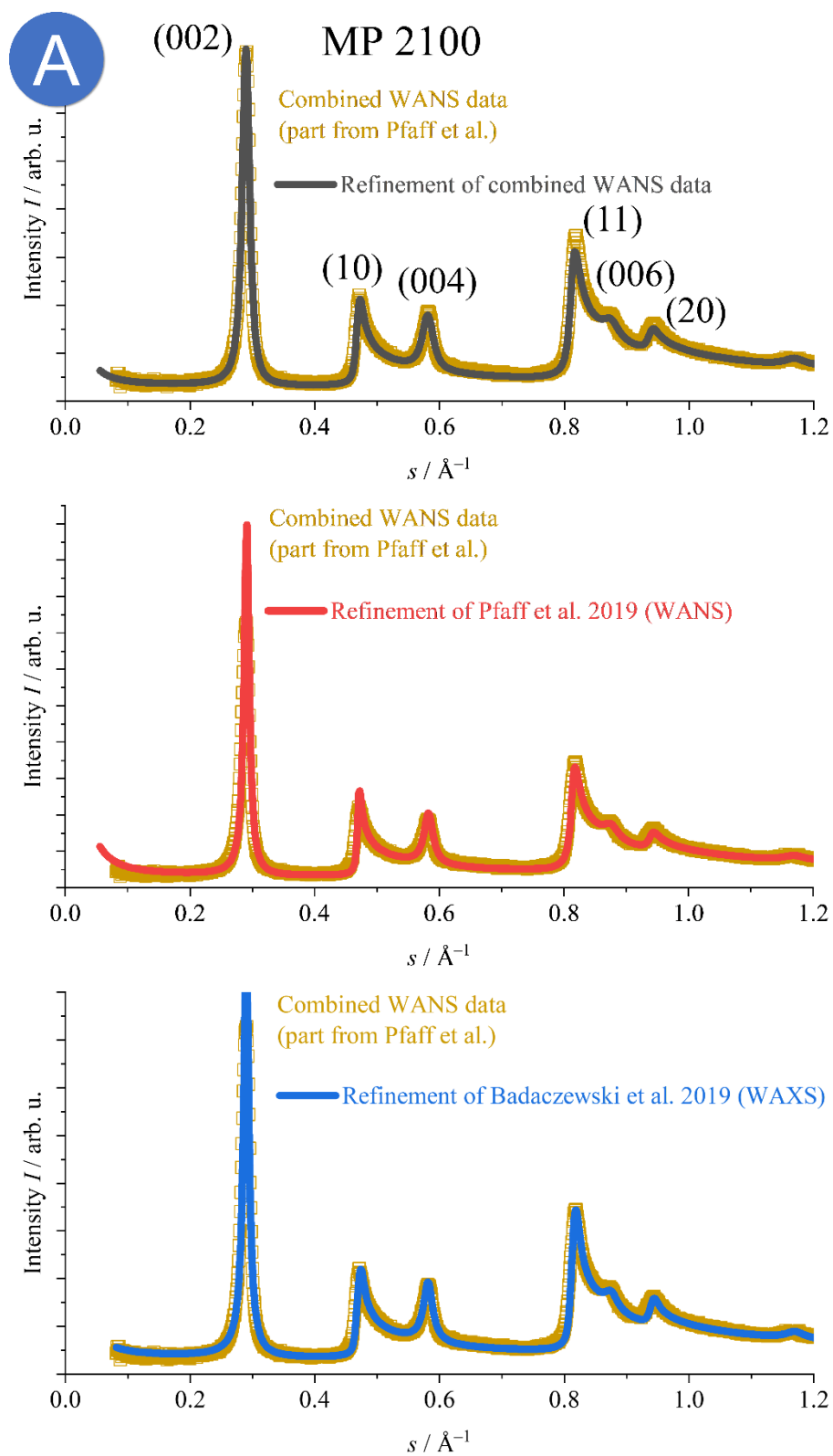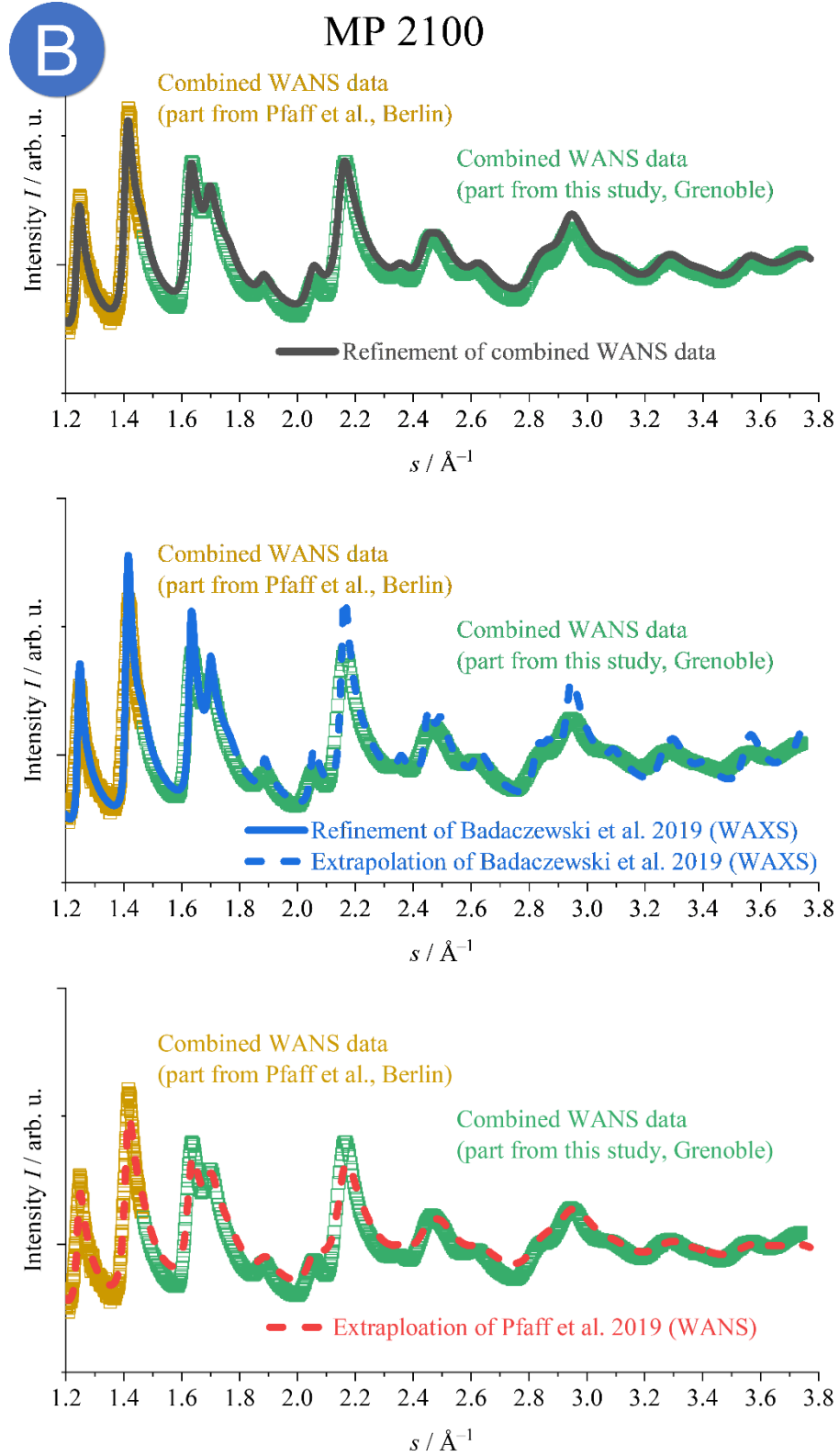
Figure S15   A: Zoom in the WAXS region ($s < 1.2$ Å^{-1}) of Figure 10 of the main article. It is seen that the fitting in the WANS study from 2019 deviates at small s, due to the different resolutions of the setups as HZB and ILL beamlines. B: Zoom in the WANS region ($s > 1.2$ Å^{-1}) of Figure 10 of the main article. It is seen that the fitting in the WANS study from 2019 deviates at large s, due to the different results for the intralayer structure, which is caused by the limited measurement range in this prior study.
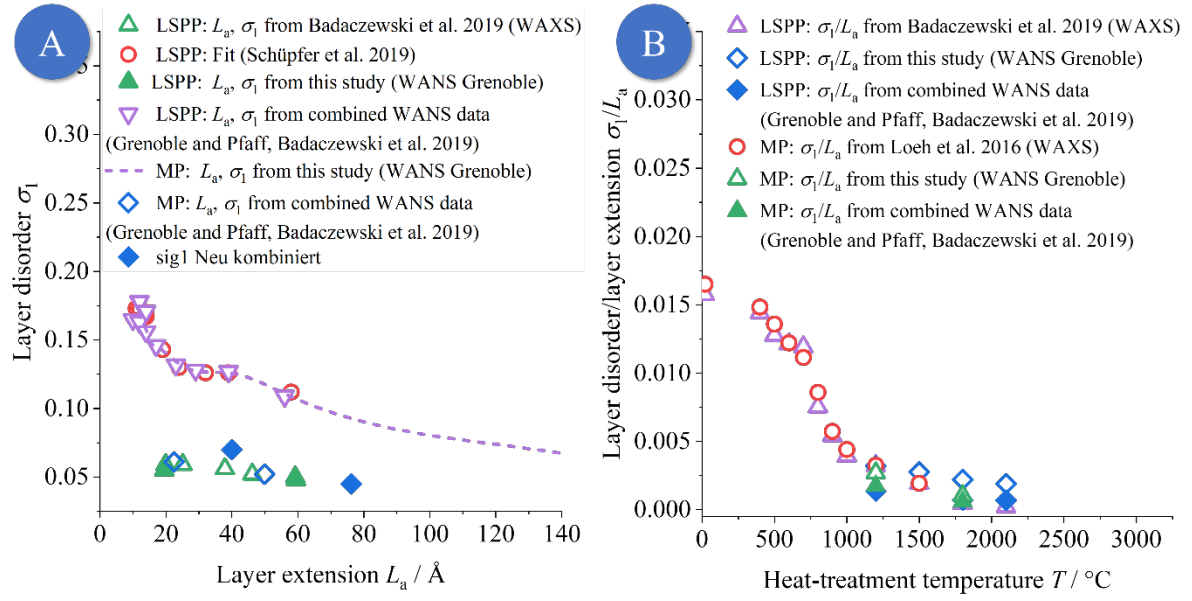
Figure S16 Even if both, σ_1 and L_a for the mesophase pitch (MP) and low softening-point pitch (LSPP) temperature series determined by WANS are much smaller compared to WAXS results, the ratio of σ_1/L_a does not change over the whole temperature range. A similar figure for the resins can be found in the main article as Figure 9.
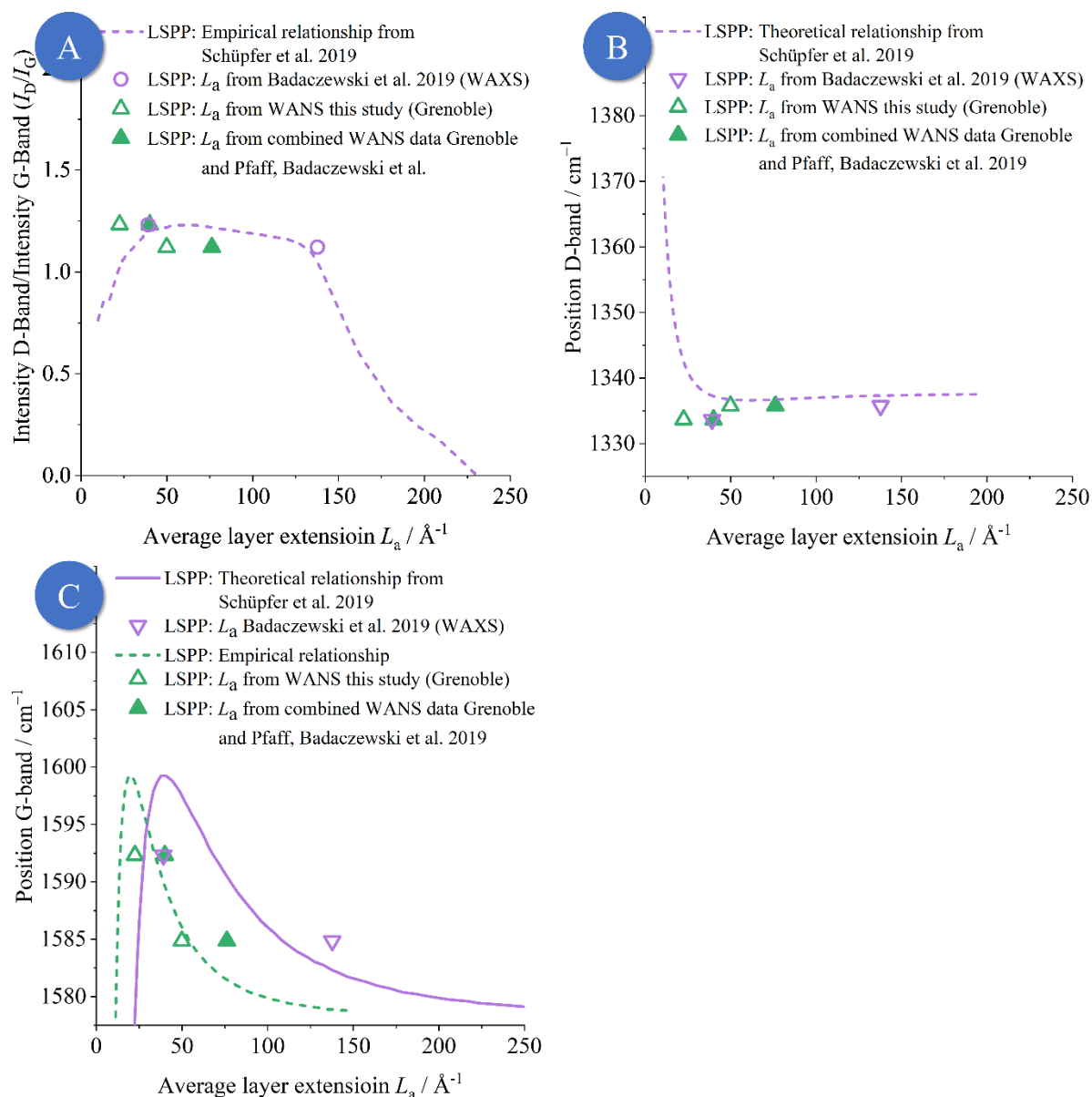
Figure S17 A: The intensity quotient between the D- and G-band (I_D/I_G) for the low softening-point pitch (LSPP) were fitted by Schüpfer et al. using L_a determined from data from Badaczewski et al. [1] Even if L_a is now different, the results from the WANS measurements still fits the fit. B: The position of the D-band is still lower than the theoretical value for these resins. It seems, that in general the theoretical calculations are not valid for (disordered) glassy carbon. C: The theoretical position of the G-band does fit the measured values for both, WAXS and WANS measurements. Even if the layer extension alters, it still fits the theoretical position. Both positions were calculated using the Campbell-Fauchet modelling as described by Schüpfer et al. [6–8] A similar figure for the resins can be found in the main article as Figure 13.
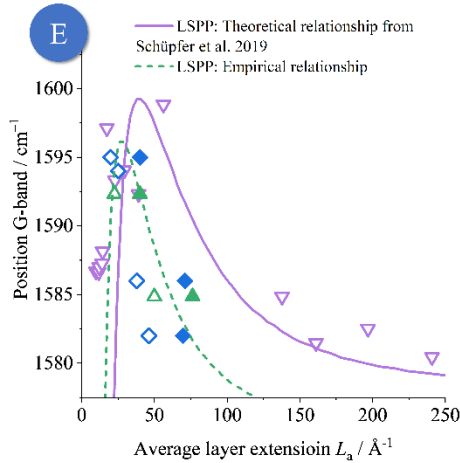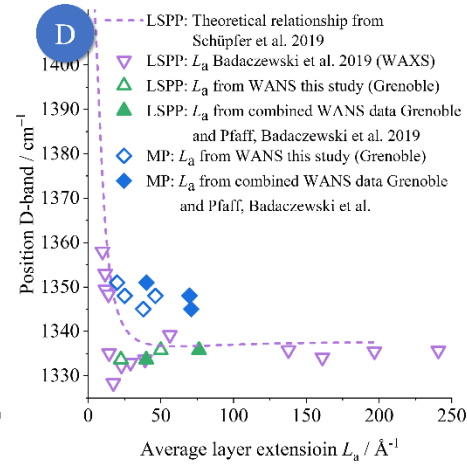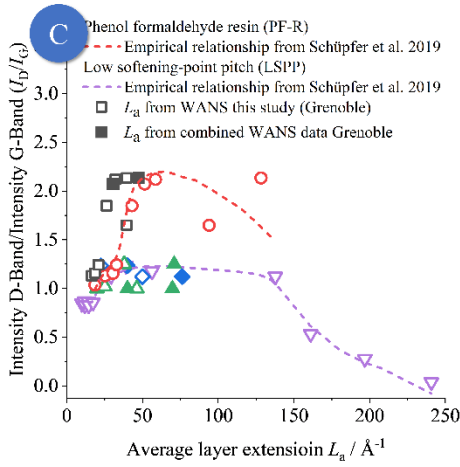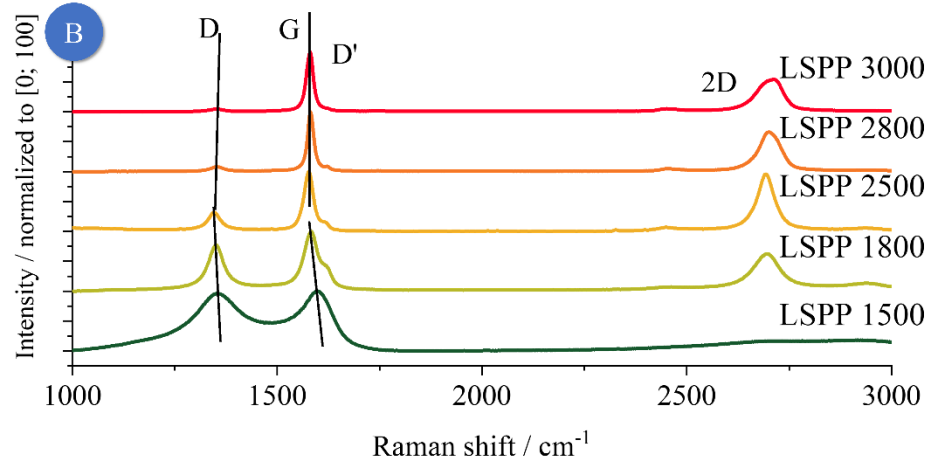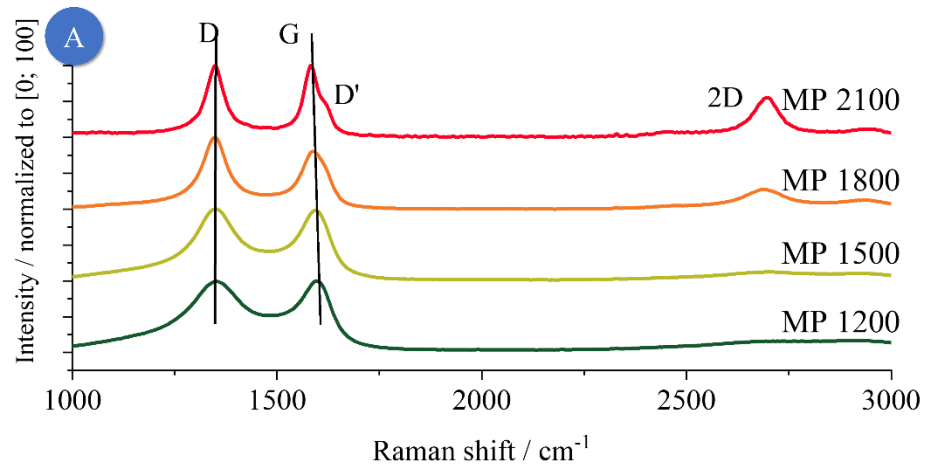
Figure S18   A/B: Measured Raman data for the mesophase and low softening-point pitch (MP/LSPP) temperature series. All samples show increasing 2D and D' bands and a higher G/D ratio at higher heat-treatment temperature, which are clear indicators for a higher degree of graphitization [6,9]. C: The intensity quotient between the D- and G-band (I_D/I_G) for the low softening-point pitch (LSPP) were fitted by Schüpfer et al. using L_a determined from data from Badaczewski et al. [1] from the MP-series. Even if L_a is now different, the results from the WANS measurements still fits the fit. D: The position of the D-band is still lower than the theoretical value for these resins. It seems, that in general the theoretical calculations are not valid for (disordered) glassy carbon. E: The theoretical position of the G-band does fit the measured values for both, WAXS and WANS measurements. Even if the layer extension alters, it still fits the theoretical position. Both positions were calculated using the Campbell-Fauchet modelling as described by Schüpfer et al. [6–8] A similar figure for the resins can be found in the main article as Figure 13.

S6. Calculation of the correlation function $P(r)$ from the layer size (L_a) and disorder (σ_1)

In order to obtain a simpler phenomenological understanding of the layer disorder parameter σ_1 (also in relation to the layer extension L_a), the layer correlation function $P(r)$ from Ruland & Smarsly [4] can be considered. This function describes the probability that an atom at a distance r (in real space) is exactly in the same position as in a graphene layer. The resulting function $P(r)$ is the multiplication of the influence through the finite layer size ($P_L(r)$) and the layer disorder ($P_D(r)$):

$$P(r) = P_L(r) \cdot P_D(r) \tag{9}$$

The correlation function for the finite layer size $P_L(r)$ can be calculated by

$$P_L(r) = \Gamma(v + 1)^{-1} \cdot [\Gamma(v + 1, \alpha \cdot r) - \alpha \cdot r \cdot \Gamma(v, \alpha \cdot r)] \tag{10}$$

using the complete ($\Gamma(x)$) and the incomplete ($\Gamma(a, x)$) gamma functions and the parameters v and α, which are related to the average layer size by $L_a = (v + 1)/\alpha$.

For the disorder, $P_D(r)$ can be calculated using the standard deviation of the next-neighbor-distribution (σ_1) and the average C-C bond for a given (hk)-reflection:

$$P_D(r) = \exp[-2 \cdot \pi^2 \cdot 2/(3 \cdot l_{cc}) \cdot r \cdot s_{hk}^2] \tag{11}$$

$$s_{hk} = \sqrt{h^2 + k^2 + h \cdot k} \cdot \frac{2}{3 \cdot l_{cc}} \tag{12}$$

In Figure S19, different plots for $P_D(r)$, $P_L(r)$ and $P(r)$ are shown. In A, the $P_D(r)$ for the phenol-formaldehyde resin (PF-R) temperature series shows a clear tendency for increasing heat-treatment temperatures, in particular $P_D(r)$ becomes higher for higher temperatures, which means a higher ordered structure. Nevertheless, the function is continuous decreasing for higher values of r, which indicates, that some disorder is present in the graphene layers. But however, even for high distances of 100 Å (= 10 nm), $P_D(r) > 0.75$, which indicates, that the layer structure is very similar to graphene and a high degree of long-range order is present even for lower heat-treatment temperatures. Additionally, a comparison of $P_D(r)$ calculated from the results of the WANS data from Grenoble in this study (filled) to the one based on the WAXS-results from Badaczewski et al. [1] can be performed. Hence, the results for $P_D(r)$ based on the WANS-results are much higher than the one based on the WAXS-results. Moreover, the results based on the WAXS-data lead more to the assumption, that the layers are highly disordered and especially for higher distances not graphene like ($P_D(r) < 0.5$). For the more accurate results based on the WANS-data, the opposite is the case: The layers are graphene like over their whole extension and the disorder is only small.

C and D in Figure S19 compare the different precursors (phenol-formaldehyde resin (PF-R), mesophase pitch (MP) and low softening-point pitch (LSPP)) for the same temperatures. It becomes clearly, that the pitches are in general higher ordered than the resin, especially for lower heat-treatment temperatures. For higher temperatures, the differences are much smaller, which means, that the layer-order is very

similar for the pitches and the resin for 1800 °C. But even if the difference for 1200 °C is higher, it is only ~ 0.05 for $r = 100$ Å, which means, that the probability, that the atom position at 100 Å differs from the perfect graphene one is only $\sim 5\%$ higher for the resin precursor compared to the low softening-point pitch precursor. Additionally to $P_D(r)$, also $P_L(r)$ and $P(r)$ are shown in B for PF-R heat-treated at 1200 °C, 1800 °C and 3000 °C. Interestingly, the influence of $P_L(r)$ is much higher as the one for $P_D(r)$ for all temperatures and therefore, the resulting $P(r)$ function is mainly dominated from the finite-layer size ($P_L(r)$) and not from the layer disorder ($P_D(r)$).
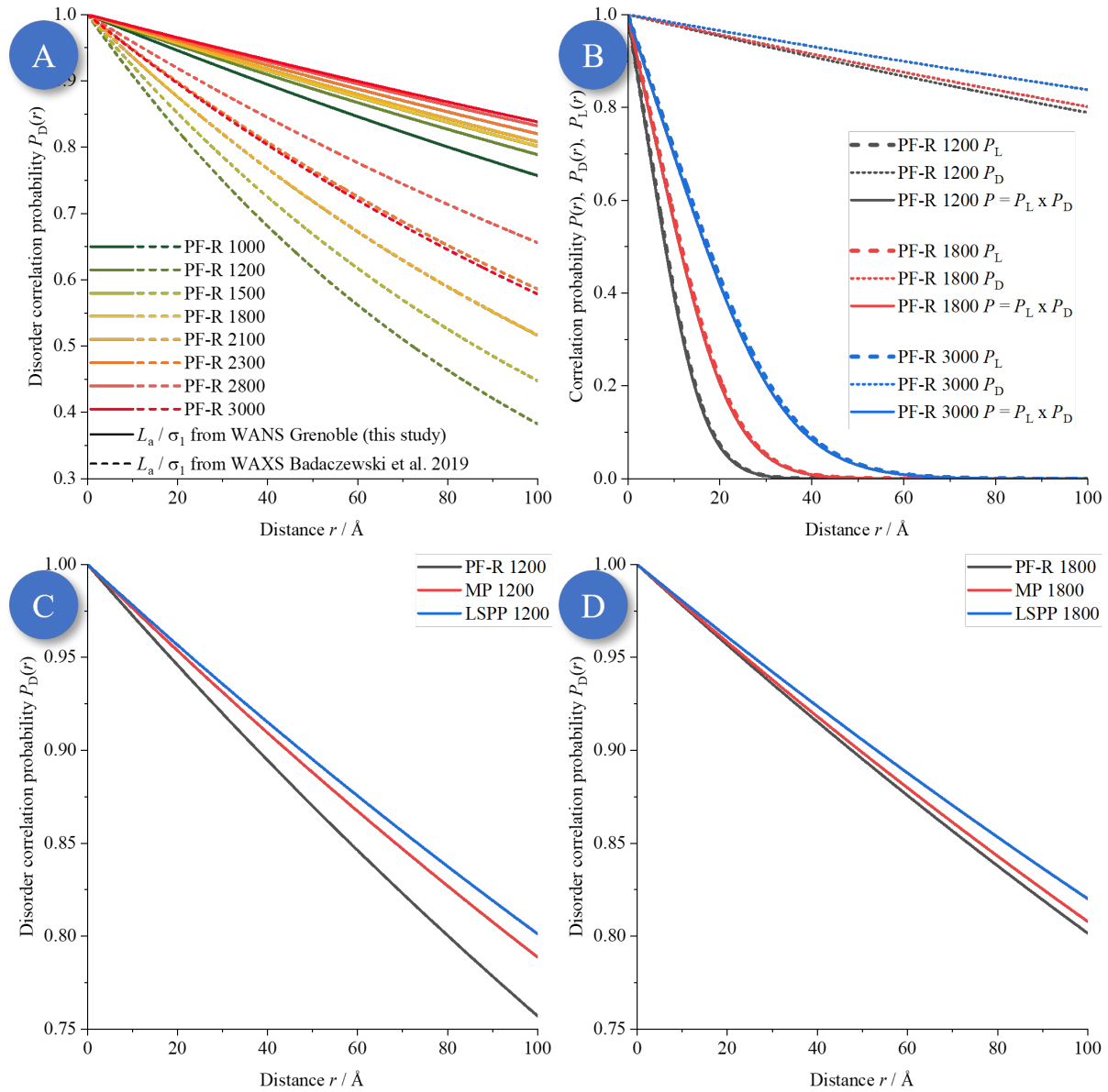
Figure S19 Plot of the layer structure correlation function ($P(r)$) based on the extension ($P_L(r)$) and disorder ($P_D(r)$). The comparison between the function based on the results from the WANS-data analysed in this study and the WAXS-data from Badaczewski et al. [1] (A) lead to the conclusion, that the layers are much more ordered as assumed and graphene like over their whole extension.

S7. Refined microstructure data

S7.1. Microstructure parameters for the phenol-formaldehyde resin (PF-R) temperature series

Table S3   Comparison of the average stack height L_c in Å for WANS data for the phenol-formaldehyde resin temperature series measured in this study, WAXS data measured by Badaczewski et al. (WAXS) [1] and WANS data measured by Pfaff, Badaczewski et al. (WANS) [2]. Additionally, the WANS data from this study from Grenoble were combined with WANS data from Pfaff, Badaczewski et al. [2]

	This study Grenoble (WANS)	Badaczewski et al. (WAXS) [1]	Pfaff, Badaczewski et al. (WANS) [2]	Combined WANS data Grenoble & Pfaff, Badaczewski et al. (WANS) [2]
Max Error	5 %	15 %	15 %	5 %
PF-R 500		9 Å		
PF-R 800		7 Å		
PF-R 1000	7.1 Å	7 Å		
PF-R 1200	10.3 Å	7 Å		
PF-R 1500	10.8 Å	8 Å		
PF-R 1800	11.8 Å	9 Å		
PF-R 2100	13.1 Å	11 Å	14 Å	11.6 Å
PF-R 2300	14.2 Å	12 Å		
PF-R 2800	19.7 Å	19 Å	23 Å	20.1 Å
PF-R 3000	20.0 Å	22 Å		

Table S4 Comparison of the average number of layers per stack *N* for WANS data for the phenol-formaldehyde resin temperature series measured in this study, WAXS data measured by Badaczewski et al. (WAXS) [1] and WANS data measured by Pfaff, Badaczewski et al. (WANS) [2]. Additionally, the WANS data from this study from Grenoble were combined with WANS data from Pfaff, Badaczewski et al. [2]

	This study Grenoble (WANS)	Badaczewski et al. (WAXS) [1]	Pfaff, Badaczewski et al. (WANS) [2]	Combined WANS data Grenoble & Pfaff, Badaczewski et al. (WANS) [2]
Max Error	7.5 %	15 %	15 %	7.5 %
PF-R 500		2.0		
PF-R 800		2.0		
PF-R 1000	1.9	2.0		
PF-R 1200	2.6	2.0		
PF-R 1500	2.7	2.2		
PF-R 1800	3.0	2.4		
PF-R 2100	3.4	3.0	4	3.3
PF-R 2300	3.7	3.4		
PF-R 2800	5.4	5.6	7	5.8
PF-R 3000	5.5	6.8		

Table S5   Comparison of the average stack height $\overline{a_3}$ in Å for WANS data for the phenol-formaldehyde resin temperature series measured in this study, WAXS data measured by Badaczewski et al. (WAXS) [1] and WANS data measured by Pfaff, Badaczewski et al. (WANS) [2]. Additionally, the WANS data from this study from Grenoble were combined with WANS data from Pfaff, Badaczewski et al. [2]

	This study Grenoble (WANS)	Badaczewski et al. (WAXS) [1]	Pfaff, Badaczewski et al. (WANS) [2]	Combined WANS data Grenoble & Pfaff, Badaczewski et al. (WANS) [2]
Max Error	0.1 %	2 %	2 %	0.1 %
PF-R 500		4.39 Å		
PF-R 800		3.59 Å		
PF-R 1000	3.68 Å	3.58 Å		
PF-R 1200	3.98 Å	3.58 Å		
PF-R 1500	3.95 Å	3.56 Å		
PF-R 1800	3.89 Å	3.50 Å		
PF-R 2100	3.83 Å	3.49 Å	3.56 Å	3.05 Å
PF-R 2300	3.80 Å	3.46 Å		
PF-R 2800	3.67 Å	3.44 Å	3.48 Å	3.46 Å
PF-R 3000	3.66 Å	3.39 Å		

Table S6   Comparison of the minimal stack height $a_{3\,\text{min}}$ in Å in Å for WANS data for the phenol-formaldehyde resin temperature series measured in this study, WAXS data measured by Badaczewski et al. (WAXS) [1] and WANS data measured by Pfaff, Badaczewski et al. (WANS) [2]. Additionally, the WANS data from this study from Grenoble were combined with WANS data from Pfaff, Badaczewski et al. [2]

	This study Grenoble (WANS)	Badaczewski et al. (WAXS) [1] **Not given**	Pfaff, Badaczewski et al. (WANS) [2]	Combined WANS data Grenoble & Pfaff, Badaczewski et al. (WANS) [2]
Max Error	2 %		12 %	2 %
PF-R 500				
PF-R 800				
PF-R 1000	3.12 Å			
PF-R 1200	3.21 Å			
PF-R 1500	3.24 Å			
PF-R 1800	3.32 Å			
PF-R 2100	3.36 Å		3.16 Å	2.74 Å
PF-R 2300	3.38 Å			
PF-R 2800	3.39 Å		3.30 Å	3.08 Å
PF-R 3000	3.39 Å			

Table S7   Comparison of the standard deviation of the layer distance σ_3 in Å for WANS data for the phenol-formaldehyde resin temperature series measured in this study, WAXS data measured by Badaczewski et al. (WAXS) [1] and WANS data measured by Pfaff, Badaczewski et al. (WANS) [2]. Additionally, the WANS data from this study from Grenoble were combined with WANS data from Pfaff, Badaczewski et al. [2]

	This study Grenoble (WANS)	Badaczewski et al. (WAXS) [1]	Pfaff, Badaczewski et al. (WANS) [2]	Combined WANS data Grenoble & Pfaff, Badaczewski et al. (WANS) [2]
Max Error	3.3 %	10 %	10 %	3.3 %
PF-R 500		1.26 Å		
PF-R 800		0.47 Å		
PF-R 1000	0.49 Å (fitting problem, 1 Å assumed)	0.35 Å		
PF-R 1200	1 Å (max fit value)	0.28 Å		
PF-R 1500	1 Å (max fit value)	0.27 Å		
PF-R 1800	1 Å (max fit value)	0.24 Å		
PF-R 2100	1 Å (max fit value)	0.22 Å	0.44 Å	0.32 Å
PF-R 2300	1 Å (max fit value)	0.21 Å		
PF-R 2800	0.86 Å	0.16 Å	0.25 Å	0.2 Å
PF-R 3000	0.83 Å	0.17 Å		

Table S8   Comparison of the homogeneity of the stacks η for WANS data for the phenol-formaldehyde resin temperature series measured in this study, WAXS data measured by Badaczewski et al. (WAXS) [1] and WANS data measured by Pfaff, Badaczewski et al. (WANS) [2]. Additionally, the WANS data from this study from Grenoble were combined with WANS data from Pfaff, Badaczewski et al. [2]

	This study Grenoble (WANS)	Badaczewski et al. (WAXS) [1]	Pfaff, Badaczewski et al. (WANS) [2]	Combined WANS data Grenoble & Pfaff, Badaczewski et al. (WANS) [2]
Max Error	0.3 %	5 %	5 %	0.3 %
PF-R 500		1 (max value)		
PF-R 800		0.90		
PF-R 1000	0.94	0.95		
PF-R 1200	0.95	0.89		
PF-R 1500	0.96	0.82		
PF-R 1800	0.95	0.92		
PF-R 2100	0.96	0.89	0.86	0.87
PF-R 2300	0.98	0.93		
PF-R 2800	1 (max value)	0.95	0.93	0.94
PF-R 3000	1 (max value)	0.94		

Table S9   Comparison of the average layer extension L_a in Å for WANS data for the phenol-formaldehyde resin temperature series measured in this study, WAXS data measured by Badaczewski et al. (WAXS) [1] and WANS data measured by Pfaff, Badaczewski et al. (WANS) [2].

	This study Grenoble (WANS)	Badaczewski et al. (WAXS) [1]	Pfaff, Badaczewski et al. (WANS) [2]	Combined WANS data Grenoble & Pfaff, Badaczewski et al. (WANS) [2]
Max Error	10 %	15 %	15 %	10 %
PF-R 500		7 Å		
PF-R 800		19 Å		
PF-R 1000	16.4 Å	25 Å		
PF-R 1200	18.7 Å	30 Å		
PF-R 1500	21.0 Å	33 Å		
PF-R 1800	26.2 Å	43 Å		
PF-R 2100	29.9 Å	51 Å	40 Å	31.0 Å
PF-R 2300	32.1 Å	59 Å		
PF-R 2800	39.5 Å	87 Å	51 Å	47.4 Å
PF-R 3000	39.5 Å	124 Å		

Table S10 Comparison of the average C-C bond length l_{cc} for WANS data for the phenol-formaldehyde resin temperature series measured in this study, WAXS data measured by Badaczewski et al. (WAXS) [1] and WANS data measured by Pfaff, Badaczewski et al. (WANS) [2]. Additionally, the WANS data from this study from Grenoble were combined with WANS data from Pfaff, Badaczewski et al. [2]

	This study Grenoble (WANS)	Badaczewski et al. (WAXS) [1]	Pfaff, Badaczewski et al. (WANS) [2]	Combined WANS data Grenoble & Pfaff, Badaczewski et al. (WANS) [2]
Max Error	0.1 %	0.4 %	0.4 %	0.1 %
PF-R 500		1.422 Å		
PF-R 800		1.410 Å		
PF-R 1000	1.4139 Å	1.408 Å		
PF-R 1200	1.4136 Å	1.408 Å		
PF-R 1500	1.4140 Å	1.410 Å		
PF-R 1800	1.4150 Å	1.412 Å		
PF-R 2100	1.4156 Å	1.413 Å	1.413 Å	1.4149 Å
PF-R 2300	1.4164 Å	1.413 Å		
PF-R 2800	1.4177 Å	1.414 Å	1.419 Å	1.4175 Å
PF-R 3000	1.4179 Å	1.402 Å		

Table S11   Comparison of the layer disorder σ_1 for WANS data for the phenol-formaldehyde resin temperature series measured in this study, WAXS data measured by Badaczewski et al. (WAXS) [1] and WANS data measured by Pfaff, Badaczewski et al. (WANS) [2]. Additionally, the WANS data from this study from Grenoble were combined with WANS data from Pfaff, Badaczewski et al. [2]

	This study Grenoble (WANS)	Badaczewski et al. (WAXS) [1]	Pfaff, Badaczewski et al. (WANS) [2]	Combined WANS data Grenoble & Pfaff, Badaczewski et al. (WANS) [2]
Max Error	2 %	12 %	12 %	2 %
PF-R 500		0.18		
PF-R 800		0.14		
PF-R 1000	0.065	0.12		
PF-R 1200	0.060	0.12		
PF-R 1500	0.058	0.11		
PF-R 1800	0.058	0.10		
PF-R 2100	0.057	0.10	0.067	0.056
PF-R 2300	0.055	0.09		
PF-R 2800	0.053	0.08	0.047	0.052
PF-R 3000	0.052	0.09		

Table S12 Comparison of the polydispersity of the layer extension stack height κ_a for WANS data for the phenol-formaldehyde resin temperature series measured in this study, WAXS data measured by Badaczewski et al. (WAXS) [1] and WANS data measured by Pfaff, Badaczewski et al. (WANS) [2]. In general, is κ_a fixed to a fixed value $\kappa_a = 1/v$. Additionally, the WANS data from this study from Grenoble were combined with WANS data from Pfaff, Badaczewski et al. [2]

	This study Grenoble (WANS)	Badaczewski et al. (WAXS) [1]	Pfaff, Badaczewski et al. (WANS) [2]	Combined WANS data Grenoble & Pfaff, Badaczewski et al. (WANS) [2]
Max Error	0 % ($v = 7$)	0 % ($v = 4$)	0 % ($v = 4$)	0 % ($v = 7$)
PF-R 500		0.25		
PF-R 800		0.25		
PF-R 1000	0.14	0.25		
PF-R 1200	0.14	0.25		
PF-R 1500	0.14	0.25		
PF-R 1800	0.14	0.25		
PF-R 2100	0.14	0.25	0.25	0.14
PF-R 2300	0.14	0.25		
PF-R 2800	0.14	0.25	0.25	0.14
PF-R 3000	0.14	0.25		

Table S13   Comparison of the polydispersity of the stack height κ_c for WANS data for the phenol-formaldehyde resin temperature series measured in this study, WAXS data measured by Badaczewski et al. (WAXS) [1] and WANS data measured by Pfaff, Badaczewski et al. (WANS) [2]. Additionally, the WANS data from this study from Grenoble were combined with WANS data from Pfaff, Badaczewski et al. [2]

	This study Grenoble (WANS)	Badaczewski et al. (WAXS) [1]	Pfaff, Badaczewski et al. (WANS) [2]	Combined WANS data Grenoble & Pfaff, Badaczewski et al. (WANS) [2]
Max Error	15 %	15 %	15 %	15 %
PF-R 500		0.45		
PF-R 800		0.39		
PF-R 1000	0.45	0.39		
PF-R 1200	0.39	0.38		
PF-R 1500	0.39	0.38		
PF-R 1800	0.38	0.37		
PF-R 2100	0.38	0.39	0.37	0.36
PF-R 2300	0.37	0.37		
PF-R 2800	0.39		0.49	0.55
PF-R 3000	0.37			

S7.2. Microstructure parameters for the mesophase pitch (MP) temperature series

Table S14 Comparison of the average stack height L_c in Å for WANS data for the phenol-formaldehyde resin temperature series measured in this study, WAXS data measured by Badaczewski et al. (WAXS) [1] and WANS data measured by Pfaff, Badaczewski et al. (WANS) [2]. Additionally, the WANS data from this study from Grenoble were combined with WANS data from Pfaff, Badaczewski et al. [2]

	This study Grenoble (WANS)	Loeh et al. (WAXS) [3]	Badaczewski et al. (WAXS) [1]	Pfaff, Badaczewski et al. (WANS) [2]	Combined WANS data Grenoble & Pfaff, Badaczewski et al. (WANS) [2]
Max Error	5 %	15 %	15 %	15 %	5 %
MP 20		11 Å			
MP 400		12 Å			
MP 500		28 Å	18 Å		
MP 600		17 Å			
MP 700		16 Å			
MP 800		12 Å	11 Å		
MP 900		12 Å			
MP 1000		14 Å	12 Å		
MP 1200	17.3 Å	18 Å	15 Å	18 Å	19.5 Å
MP 1500	18.9 Å	39 Å	27 Å		
MP 1800	23.6 Å	151 Å	53 Å	44 Å	59.2 Å
MP 2100	25.0 Å	198 Å	84 Å	81 Å	59.4 Å

Table S15 Comparison of the average number of layers per stack N for WANS data for the phenol-formaldehyde resin temperature series measured in this study, WAXS data measured by Badaczewski et al. (WAXS) [1] and WANS data measured by Pfaff, Badaczewski et al. (WANS) [2]. Additionally, the WANS data from this study from Grenoble were combined with WANS data from Pfaff, Badaczewski et al. [2]

	This study Grenoble (WANS)	Loeh et al. (WAXS) [3]	Badaczewski et al. (WAXS) [1]	Pfaff, Badaczewski et al. (WANS) [2]	Combined WANS data Grenoble & Pfaff, Badaczewski et al. (WANS) [2]
Max Error	5 %	15 %	15 %	15 %	5 %
MP 20		3			
MP 400		4			
MP 500		8	5.1		
MP 600		5			
MP 700		5			
MP 800		4	3.3		
MP 900		4			
MP 1000		4	3.5		
MP 1200	4.7	5	4.4	5.1	5.6
MP 1500	5.4	11	7.7		
MP 1800	6.8	44	15.5	12.7	17.1
MP 2100	7.3	58	24.5	23.0	17.2

Table S16 Comparison of the average stack height $\overline{a_3}$ in Å for WANS data for the phenol-formaldehyde resin temperature series measured in this study, WAXS data measured by Badaczewski et al. (WAXS) [1] and WANS data measured by Pfaff, Badaczewski et al. (WANS) [2]. Additionally, the WANS data from this study from Grenoble were combined with WANS data from Pfaff, Badaczewski et al. [2]

	This study Grenoble (WANS)	Loeh et al. (WAXS) [3]	Badaczewski et al. (WAXS) [1]	Pfaff, Badaczewski et al. (WANS) [2]	Combined WANS data Grenoble & Pfaff, Badaczewski et al. (WANS) [2]
Max Error	5 %	15 %	15 %	15 %	5 %
MP 20		3.52 Å			
MP 400		3.51 Å			
MP 500		3.46 Å	3.46 Å		
MP 600		3.46 Å			
MP 700		3.45 Å			
MP 800		3.44 Å	3.46 Å		
MP 900		3.44 Å			
MP 1000		3.46 Å	3.47 Å		
MP 1200	3.69 Å	3.46 Å	3.49 Å	3.53 Å	3.5 Å
MP 1500	3.52 Å	3.44 Å	3.47 Å		
MP 1800	3.47 Å	3.42 Å	3.44 Å	3.47 Å	3.45 Å
MP 2100	3.45 Å	3.41 Å	3.44 Å	3.45 Å	3.45 Å

Table S17   Comparison of the minimal stack height $a_{3\,min}$ in Å in Å for WANS data for the phenol-formaldehyde resin temperature series measured in this study, WAXS data measured by Badaczewski et al. (WAXS) [1] and WANS data measured by Pfaff, Badaczewski et al. (WANS) [2]. Additionally, the WANS data from this study from Grenoble were combined with WANS data from Pfaff, Badaczewski et al. [2]

	This study Grenoble (WANS)	Loeh et al. (WAXS) [3]	Badaczewski et al. (WAXS) [1]	Pfaff, Badaczewski et al. (WANS) [2]	Combined WANS data Grenoble & Pfaff, Badaczewski et al. (WANS) [2]
Max Error	5 %	15 %	15 %	15 %	5 %
MP 20		3.52 Å			
MP 400		3.51 Å			
MP 500		3.46 Å	3 Å (min fit value)		
MP 600		3.46 Å			
MP 700		3.45 Å			
MP 800		3.44 Å	3 Å (min fit value)		
MP 900		3.44 Å			
MP 1000		3.46 Å	3.24 Å		
MP 1200	3.28 Å	3.46 Å	3.08 Å		3.30 Å
MP 1500	3.27 Å	3.44 Å	3.11 Å		
MP 1800	3.37 Å	3.42 Å	3.05 Å		3.33 Å
MP 2100	3.39 Å	3.41 Å	3.19 Å	3.34	3.34 Å

Table S18   Comparison of the standard deviation of the layer distance σ_3 in Å for WANS data for the phenol-formaldehyde resin temperature series measured in this study, WAXS data measured by Badaczewski et al. (WAXS) [1] and WANS data measured by Pfaff, Badaczewski et al. (WANS) [2]. Additionally, the WANS data from this study from Grenoble were combined with WANS data from Pfaff, Badaczewski et al. [2]

	This study Grenoble (WANS)	Loeh et al. (WAXS) [3]	Badaczewski et al. (WAXS) [1]	Pfaff, Badaczewski et al. (WANS) [2]	Combined WANS data Grenoble & Pfaff, Badaczewski et al. (WANS) [2]
Max Error	5 %	15 %	15 %	15 %	5 %
MP 20		0.32 Å			
MP 400		0.30 Å			
MP 500		0.26 Å	0.26 Å		
MP 600		0.25 Å			
MP 700		0.26 Å			
MP 800		0.27 Å	0.32 Å		
MP 900		0.24 Å			
MP 1000		0.26 Å	0.27 Å		
MP 1200	0.63 Å	0.22 Å	0.27 Å	0.42 Å	0.4 Å
MP 1500	0.31 Å	0.19 Å	0.23 Å		
MP 1800	0.18 Å	0.11 Å	0.15 Å	0.22 Å	0.14 Å
MP 2100	0.10 Å	0.10 Å	0.13 Å	0.14 Å	0.14 Å

Table S19 Comparison of the homogeneity of the stacks η for WANS data for the phenol-formaldehyde resin temperature series measured in this study, WAXS data measured by Badaczewski et al. (WAXS) [1] and WANS data measured by Pfaff, Badaczewski et al. (WANS) [2]. Additionally, the WANS data from this study from Grenoble were combined with WANS data from Pfaff, Badaczewski et al. [2]

	This study Grenoble (WANS)	Loeh et al. (WAXS) [3]	Badaczewski et al. (WAXS) [1]	Pfaff, Badaczewski et al. (WANS) [2]	Combined WANS data Grenoble & Pfaff, Badaczewski et al. (WANS) [2]
Max Error	5 %	15 %	15 %	15 %	5 %
MP 20		0.77			
MP 400		0.71			
MP 500		0.70	0.68		
MP 600		0.75			
MP 700		0.76			
MP 800		0.96	1 (max value)		
MP 900		0.97	1 (max value)		
MP 1000		1 (max value)	1 (max value)		
MP 1200	1 (max value)	1 (max value)	1 (max value)		1 (max value)
MP 1500	1 (max value)	1 (max value)	0.97		
MP 1800	1 (max value)	0.97	0.97		0.99
MP 2100	1 (max value)	0.99	0.96	0.99	0.99

Table S20 Comparison of the average layer extension L_a in Å for WANS data for the phenol-formaldehyde resin temperature series measured in this study, WAXS data measured by Badaczewski et al. (WAXS) [1] and WANS data measured by Pfaff, Badaczewski et al. (WANS) [2]. Additionally, the WANS data from this study from Grenoble were combined with WANS data from Pfaff, Badaczewski et al. [2]

	This study Grenoble (WANS)	Loeh et al. (WAXS) [3]	Badaczewski et al. (WAXS) [1]	Pfaff, Badaczewski et al. (WANS) [2]	Combined WANS data Grenoble & Pfaff, Badaczewski et al. (WANS) [2]
Max Error	5 %	15 %	15 %	15 %	5 %
MP 20		11 Å			
MP 400		12 Å			
MP 500		13 Å	13 Å		
MP 600		14 Å			
MP 700		14 Å			
MP 800		19 Å	16 Å		
MP 900		24 Å			
MP 1000		32 Å	33 Å		
MP 1200	19.9 Å	39 Å	34 Å	34 Å	19.5 Å
MP 1500	25.1 Å	58 Å	47 Å		
MP 1800	37.9 Å	148 Å	85 Å	48 Å	59.2 Å
MP 2100	46.2 Å	210 Å	130 Å	77 Å	59.4 Å

Table S21 Comparison of the average C-C bond length l_{cc} for WANS data for the phenol-formaldehyde resin temperature series measured in this study, WAXS data measured by Badaczewski et al. (WAXS) [1] and WANS data measured by Pfaff, Badaczewski et al. (WANS) [2]. Additionally, the WANS data from this study from Grenoble were combined with WANS data from Pfaff, Badaczewski et al. [2]

	This study Grenoble (WANS)	Loeh et al. (WAXS) [3]	Badaczew-ski et al. (WAXS) [1]	Pfaff, Bada-czewski et al. (WANS) [2]	Combined WANS data Grenoble & Pfaff, Bada-czewski et al. (WANS) [2]
Max Error	5 %	15 %	15 %	15 %	5 %
MP 20		1.414 Å			
MP 400		1.417 Å			
MP 500		1.412 Å	1.413 Å		
MP 600		1.413 Å			
MP 700		1.412 Å			
MP 800		1.412 Å	1.409 Å		
MP 900		1.411 Å			
MP 1000		1.413 Å	1.413 Å		
MP 1200	1.4163 Å	1.413 Å	1.413 Å	1.417 Å	1.4187 Å
MP 1500	1.4177 Å	1.415 Å	1.414 Å		
MP 1800	1.4190 Å	1.420 Å	1.416 Å	1.420 Å	1.4203 Å
MP 2100	1.4198 Å	1.421 Å	1.417 Å	1.417 Å	1.4203 Å

Table S22 Comparison of the layer disorder σ_1 for WANS data for the phenol-formaldehyde resin temperature series measured in this study, WAXS data measured by Badaczewski et al. (WAXS) [1] and WANS data measured by Pfaff, Badaczewski et al. (WANS) [2]. Additionally, the WANS data from this study from Grenoble were combined with WANS data from Pfaff, Badaczewski et al. [2]

	This study Grenoble (WANS)	Loeh et al. (WAXS) [3]	Badaczew-ski et al. (WAXS) [1]	Pfaff, Bada-czewski et al. (WANS) [2]	Combined WANS data Grenoble & Pfaff, Bada-czewski et al. (WANS) [2]
Max Error	5 %	15 %	15 %	15 %	5 %
MP 20		0.173			
MP 400		0.173			
MP 500		0.166	0.16		
MP 600		0.170			
MP 700		0.167			
MP 800		0.143	0.13		
MP 900		0.130			
MP 1000		0.126	0.13		
MP 1200	0.059	0.126	0.12	0.059	0.055
MP 1500	0.059	0.112	0.10		
MP 1800	0.056	0.065	0.08	0.050	0.050
MP 2100	0.052	0.045	0.07	0.036	0.048

Table S23 Comparison of the polydispersity of the layer extension stack height κ_a for WANS data for the phenol-formaldehyde resin temperature series measured in this study, WAXS data measured by Badaczewski et al. (WAXS) [1] and WANS data measured by Pfaff, Badaczewski et al. (WANS) [2]. In general, is κ_a fixed to a fixed value $\kappa_a = 1/v$. Additionally, the WANS data from this study from Grenoble were combined with WANS data from Pfaff, Badaczewski et al. [2]

	This study Grenoble (WANS)	Loeh et al. (WAXS) [3]	Badaczewski et al. (WAXS) [1]	Pfaff, Badaczewski et al. (WANS) [2]	Combined WANS data Grenoble & Pfaff, Badaczewski et al. (WANS) [2]
Max Error	5 %	15 %	15 %	15 %	5 %
MP 20		0.25			
MP 400		0.25			
MP 500		0.25	0.25		
MP 600		0.25			
MP 700		0.25			
MP 800		0.25	0.25		
MP 900		0.25			
MP 1000		0.25	0.25		
MP 1200	0.14	0.25	0.25		0.14
MP 1500	0.14	0.25	0.25		
MP 1800	0.14	0.25	0.25		0.14
MP 2100	0.14	0.25	0.25	0.25	0.14

Table S24   Comparison of the polydispersity of the stack height κ_c for WANS data for the phenol-formaldehyde resin temperature series measured in this study, WAXS data measured by Badaczewski et al. (WAXS) [1] and WANS data measured by Pfaff, Badaczewski et al. (WANS) [2]. Additionally, the WANS data from this study from Grenoble were combined with WANS data from Pfaff, Badaczewski et al. [2]

	This study Grenoble (WANS)	Loeh et al. (WAXS) [3]	Badaczewski et al. (WAXS) [1]	Pfaff, Badaczewski et al. (WANS) [2]	Combined WANS data Grenoble & Pfaff, Badaczewski et al. (WANS) [2]
Max Error	5 %	15 %	15 %	15 %	5 %
MP 20		1.24			
MP 400		1.46			
MP 500		4.05	2.22		
MP 600		4.48			
MP 700		1.74			
MP 800		1.04	1.92		
MP 900		0.66			
MP 1000		0.51	0.85		
MP 1200	0.39	0.46	0.94		0.4
MP 1500	0.4	0.53	0.46		
MP 1800	0.37	0.54	0.86		0.57
MP 2100	0.39	0.04	1	2.23	0.57

Table S25   Comparison of the average stack height L_c in Å for WANS data for the low softening-point pitch temperature series measured in this study, WAXS data measured by Badaczewski et al. (WAXS) [1] and WANS data measured by Pfaff, Badaczewski et al. (WANS) [2]. Additionally, the WANS data from this study from Grenoble were combined with WANS data from Pfaff, Badaczewski et al. [2]

	This study Grenoble (WANS)	Loeh et al. (WAXS) [1]	Pfaff, Badaczewski et al. (WANS) [2]	Combined WANS data Grenoble & Pfaff, Badaczewski et al. (WANS) [2]
Max Error	5 %	15 %	15 %	5 %
LSSP 20		9 Å		
LSSP 400		12 Å		
LSSP 500		25 Å		
LSSP 600		20 Å		
LSSP 700		15 Å		
LSSP 800		12 Å		
LSSP 900		13 Å		
LSSP 1000		13 Å		
LSSP 1200	14.6 Å	19 Å	17 Å	18.7 Å
LSSP 1500		42 Å		
LSSP 1800	25.5 Å		100 Å	74.5 Å
LSSP 2500 (Scherrer)	69.4 Å (25 % error)	140 Å	72 Å (WAXS: 130 Å)	
LSSP 2800 (Scherrer)	67.8 Å (25 % error)		77 Å (WAXS: 149 Å)	
LSSP 3000 (Scherrer)	69.5 Å (25 % error)	260 Å	78 Å (WAXS: 171 Å)	

Table S26   Comparison of the average number of layers per stack N for WANS data for the low softening-point pitch temperature series measured in this study, WAXS data measured by Badaczewski et al. (WAXS) [1] and WANS data measured by Pfaff, Badaczewski et al. (WANS) [2]. Additionally, the WANS data from this study from Grenoble were combined with WANS data from Pfaff, Badaczewski et al. [2]

	This study Grenoble (WANS)	Loeh et al. (WAXS) [1]	Pfaff, Badaczewski et al. (WANS) [2]	Combined WANS data Grenoble & Pfaff, Badaczewski et al. (WANS) [2]
Max Error	7.5 %	15 %	15 %	7.5 %
LSSP 20		3		
LSSP 400		3		
LSSP 500		7		
LSSP 600		6		
LSSP 700		4		
LSSP 800		4		
LSSP 900		4		
LSSP 1000		4		
LSSP 1200	4.1	5	5	5.3
LSSP 1500		12		
LSSP 1800	7.4		29	21.6
LSSP 2500 (Scherrer)	20.3 (25 % error)	41		
LSSP 2800 (Scherrer)	20.0 (25 % error)			
LSSP 3000 (Scherrer)	20.6 (25 % error)	77		

Table S27 Comparison of the average stack height $\overline{a_3}$ in Å for WANS data for the low softening-point pitch temperature series measured in this study, WAXS data measured by Badaczewski et al. (WAXS) [1] and WANS data measured by Pfaff, Badaczewski et al. (WANS) [2]. Additionally, the WANS data from this study from Grenoble were combined with WANS data from Pfaff, Badaczewski et al. [2]

	This study Grenoble (WANS)	Loeh et al. (WAXS) [1]	Pfaff, Badaczewski et al. (WANS) [2]	Combined WANS data Grenoble & Pfaff, Badaczewski et al. (WANS) [2]
Max Error	0.1 %	2 %	2 %	0.1 %
LSSP 20		3.55 Å		
LSSP 400		3.50 Å		
LSSP 500		3.46 Å		
LSSP 600		3.47 Å		
LSSP 700		3.44 Å		
LSSP 800		3.42 Å		
LSSP 900		3.44 Å		
LSSP 1000		3.45 Å		
LSSP 1200	3.54 Å	3.45 Å	3.48 Å	3.51 Å
LSSP 1500		3.44 Å		
LSSP 1800	3.43 Å		3.43 Å	3.45 Å
LSSP 2500 (Scherrer)	3.42 Å (2 % error)	3.41 Å		
LSSP 2800 (Scherrer)	3.39 Å (2 % error)			
LSSP 3000 (Scherrer)	3.38 Å (2 % error)	3.36 Å		

Table S28   Comparison of the minimal stack height $a_{3\ min}$ in Å in Å for WANS data for the low softening-point pitch temperature series measured in this study, WAXS data measured by Badaczewski et al. (WAXS) [1] and WANS data measured by Pfaff, Badaczewski et al. (WANS) [2]. Additionally, the WANS data from this study from Grenoble were combined with WANS data from Pfaff, Badaczewski et al. [2]

	This study Grenoble (WANS)	Loeh et al. (WAXS) [1]	Pfaff, Badaczewski et al. (WANS) [2]	Combined WANS data Grenoble & Pfaff, Badaczewski et al. (WANS) [2]
Max Error	2 %	12 %	12 %	2 %
LSSP 20		3 Å (min fit value)		
LSSP 400		3 Å (min fit value)		
LSSP 500		3 Å (min fit value)		
LSSP 600		3 Å (min fit value)		
LSSP 700		3 Å (min fit value)		
LSSP 800		3 Å (min fit value)		
LSSP 900		3 Å (min fit value)		
LSSP 1000		3 Å (min fit value)		
LSSP 1200	3.21 Å	3 Å (min fit value)	3 Å (min fit value)	3.11 Å
LSSP 1500		3 Å (min fit value)		
LSSP 1800	2.76 Å		3 Å (min fit value)	3.36 Å
LSSP 2500 (Scherrer)				
LSSP 2800 (Scherrer)				
LSSP 3000 (Scherrer)				

Table S29   Comparison of the standard deviation of the layer distance σ_3 in Å for WANS data for the low softening-point pitch temperature series measured in this study, WAXS data measured by Badaczewski et al. (WAXS) [1] and WANS data measured by Pfaff, Badaczewski et al. (WANS) [2]. Additionally, the WANS data from this study from Grenoble were combined with WANS data from Pfaff, Badaczewski et al. [2]

	This study Grenoble (WANS)	Loeh et al. (WAXS) [1]	Pfaff, Badaczewski et al. (WANS) [2]	Combined WANS data Grenoble & Pfaff, Badaczewski et al. (WANS) [2]
Max Error	3.3 %	10 %	10 %	3.3 %
LSSP 20		0.34 Å		
LSSP 400		0.28 Å		
LSSP 500		0.27 Å		
LSSP 600		0.28 Å		
LSSP 700		0.27 Å		
LSSP 800		0.24 Å		
LSSP 900		0.26 Å		
LSSP 1000		0.25 Å		
LSSP 1200	0.35 Å	0.22 Å	0.31 Å	0.36 Å
LSSP 1500		0.19 Å		
LSSP 1800	0.07 Å		0.12 Å	0.13 Å
LSSP 2500 (Scherrer)				
LSSP 2800 (Scherrer)				
LSSP 3000 (Scherrer)				

Table S30   Comparison of the homogeneity of the stacks η for WANS data for the low softening-point pitch temperature series measured in this study, WAXS data measured by Badaczewski et al. (WAXS) [1] and WANS data measured by Pfaff, Badaczewski et al. (WANS) [2]. Additionally, the WANS data from this study from Grenoble were combined with WANS data from Pfaff, Badaczewski et al. [2]

	This study Grenoble (WANS)	Loeh et al. (WAXS) [1]	Pfaff, Badaczewski et al. (WANS) [2]	Combined WANS data Grenoble & Pfaff, Badaczewski et al. (WANS) [2]
Max Error	0.3 %	5 %	5 %	0.3 %
LSSP 20		0.78		
LSSP 400		0.71		
LSSP 500		0.67		
LSSP 600		0.68		
LSSP 700		0.81		
LSSP 800		0.96		
LSSP 900		0.97		
LSSP 1000		1 (max value)		
LSSP 1200	1 (max value)	1 (max value)	1 (max value)	1 (max value)
LSSP 1500		1 (max value)		
LSSP 1800	1 (max value)		1 (max value)	0.99
LSSP 2500 (Scherrer)				
LSSP 2800 (Scherrer)				
LSSP 3000 (Scherrer)				

Table S31 Comparison of the average layer extension L_a in Å for WANS data for the low softening-point pitch temperature series measured in this study, WAXS data measured by Badaczewski et al. (WAXS) [1] and WANS data measured by Pfaff, Badaczewski et al. (WANS) [2]. Additionally, the WANS data from this study from Grenoble were combined with WANS data from Pfaff, Badaczewski et al. [2]

	This study Grenoble (WANS)	Loeh et al. (WAXS) [1]	Pfaff, Badaczewski et al. (WANS) [2]	Combined WANS data Grenoble & Pfaff, Badaczewski et al. (WANS) [2]
Max Error	10 %	15 %	15 %	10 %
LSSP 20		10 Å		
LSSP 400		12 Å		
LSSP 500		12 Å		
LSSP 600		14 Å		
LSSP 700		14 Å		
LSSP 800		17 Å		
LSSP 900		23 Å		
LSSP 1000		29 Å		
LSSP 1200	22.5 Å	39 Å	27 Å	40.0 Å
LSSP 1500		56 Å		
LSSP 1800	49.9 Å		126 Å	76.2 Å
LSSP 2500 (Scherrer)				
LSSP 2800 (Scherrer)				
LSSP 3000 (Scherrer)				

Table S32 Comparison of the average C-C bond length l_{cc} for WANS data for the low softening-point pitch temperature series measured in this study, WAXS data measured by Badaczewski et al. (WAXS) [1] and WANS data measured by Pfaff, Badaczewski et al. (WANS) [2]. Additionally, the WANS data from this study from Grenoble were combined with WANS data from Pfaff, Badaczewski et al. [2]

	This study Grenoble (WANS)	Loeh et al. (WAXS) [1]	Pfaff, Badaczewski et al. (WANS) [2]	Combined WANS data Grenoble & Pfaff, Badaczewski et al. (WANS) [2]
Max Error	0.1 %	0.4 %	0.4 %	0.1 %
LSSP 20		1.411 Å		
LSSP 400		1.414 Å		
LSSP 500		1.409 Å		
LSSP 600		1.416 Å		
LSSP 700		1.413 Å		
LSSP 800		1.409 Å		
LSSP 900		1.414 Å		
LSSP 1000		1.413 Å		
LSSP 1200	1.4176 Å	1.412 Å	1.418 Å	1.4182 Å
LSSP 1500		1.416 Å		
LSSP 1800	1.4209 Å		1.421 Å	1.4215 Å
LSSP 2500 (Scherrer)	1.4063 Å			
LSSP 2800 (Scherrer)	1.413 Å			
LSSP 3000 (Scherrer)	1.3382 Å			

Table S33 Comparison of the layer disorder σ_1 for WANS data for the low softening-point pitch temperature series measured in this study, WAXS data measured by Badaczewski et al. (WAXS) [1] and WANS data measured by Pfaff, Badaczewski et al. (WANS) [2]. Additionally, the WANS data from this study from Grenoble were combined with WANS data from Pfaff, Badaczewski et al. [2]

	This study Grenoble (WANS)	Loeh et al. (WAXS) [1]	Pfaff, Badaczewski et al. (WANS) [2]	Combined WANS data Grenoble & Pfaff, Badaczewski et al. (WANS) [2]
Max Error	2 %	12 %	12 %	2 %
LSSP 20		0.165		
LSSP 400		0.178		
LSSP 500		0.163		
LSSP 600		0.171		
LSSP 700		0.156		
LSSP 800		0.146		
LSSP 900		0.132		
LSSP 1000		0.128		
LSSP 1200	0.061	0.127	0.062	0.07
LSSP 1500		0.109		
LSSP 1800	0.052		0.032	0.045
LSSP 2500 (Scherrer)				
LSSP 2800 (Scherrer)				
LSSP 3000 (Scherrer)				

Table S34 Comparison of the polydispersity of the layer extension stack height κ_a for WANS data for the low softening-point pitch temperature series measured in this study, WAXS data measured by Badaczewski et al. (WAXS) [1] and WANS data measured by Pfaff, Badaczewski et al. (WANS) [2]. In general, is κ_a fixed to a fixed value $\kappa_a = 1/v$. Additionally, the WANS data from this study from Grenoble were combined with WANS data from Pfaff, Badaczewski et al. [2]

	This study Grenoble (WANS)	Loeh et al. (WAXS) [1]	Pfaff, Badaczewski et al. (WANS) [2]	Combined WANS data Grenoble & Pfaff, Badaczewski et al. (WANS) [2]
Max Error	0 % ($v = 7$)	0 % ($v = 4$)	0 % ($v = 4$)	0 % ($v = 7$)
LSSP 20		0.25		
LSSP 400		0.25		
LSSP 500		0.25		
LSSP 600		0.25		
LSSP 700		0.25		
LSSP 800		0.25		
LSSP 900		0.25		
LSSP 1000		0.25		
LSSP 1200	0.14	0.25	0.25	0.14
LSSP 1500		0.25		
LSSP 1800	0.14		0.25	0.14
LSSP 2500 (Scherrer)				
LSSP 2800 (Scherrer)				
LSSP 3000 (Scherrer)				

Table S35 Comparison of the polydispersity of the stack height κ_c for WANS data for the low softening-point pitch temperature series measured in this study, WAXS data measured by Badaczewski et al. (WAXS) [1] and WANS data measured by Pfaff, Badaczewski et al. (WANS) [2]. Additionally, the WANS data from this study from Grenoble were combined with WANS data from Pfaff, Badaczewski et al. [2]

	This study Grenoble (WANS)	Loeh et al. (WAXS) [1]	Pfaff, Badaczewski et al. (WANS) [2]	Combined WANS data Grenoble & Pfaff, Badaczewski et al. (WANS) [2]
Max Error	15 %	15 %	15 %	15 %
LSSP 20		1.24		
LSSP 400		1.25		
LSSP 500		3.78		
LSSP 600		2.55		
LSSP 700		1.38		
LSSP 800		1.13		
LSSP 900		0.7		
LSSP 1000		0.52		
LSSP 1200	0.44	0.43	0.63	1.67
LSSP 1500		0.46		
LSSP 1800	0.58		0.11	0.27
LSSP 2500 (Scherrer)				
LSSP 2800 (Scherrer)				
LSSP 3000 (Scherrer)				

1. Badaczewski, F.; Loeh, M.O.; Pfaff, T.; Dobrotka, S.; Wallacher, D.; Clemens, D.; Metz, J.; Smarsly, B.M. Peering into the structural evolution of glass-like carbons derived from phenolic resin by combining small-angle neutron scattering with an advanced evaluation method for wide-angle X-ray scattering. *Carbon* **2019**, *141*, 169–181, doi:10.1016/j.carbon.2018.09.025.

2. Pfaff, T.; Badaczewski, F.M.; Loeh, M.O.; Franz, A.; Hoffmann, J.-U.; Reehuis, M.; Zeier, W.G.; Smarsly, B.M. Comparative Microstructural Analysis of Nongraphitic Carbons by Wide-Angle X-ray and Neutron Scattering. *J. Phys. Chem. C* **2019**, *123*, 20532–20546, doi:10.1021/acs.jpcc.9b03590.

3. Loeh, M.O.; Badaczewski, F.; Faber, K.; Hintner, S.; Bertino, M.F.; Mueller, P.; Metz, J.; Smarsly, B.M. Analysis of thermally induced changes in the structure of coal tar pitches by an advanced evaluation method of X-ray scattering data. *Carbon* **2016**, *109*, 823–835, doi:10.1016/j.carbon.2016.08.031.

4. Ruland, W.; Smarsly, B.M. X-ray scattering of non-graphitic carbon: an improved method of evaluation. *J Appl Crystallogr* **2002**, *35*, 624–633, doi:10.1107/S0021889802011007.

5. Osswald, O.; Smarsly, B.M. OctCarb - A GNU Octave Script for the Analysis and Evaluation of Wide-Angle Scattering Data of Non-Graphitic Carbons. *C* **2022**, *8(4)*, doi:10.3390/c8040078.

6. Schüpfer, D.B.; Badaczewski, F.; Guerra-Castro, J.M.; Hofmann, D.M.; Heiliger, C.; Smarsly, B.M.; Klar, P.J. Assessing the structural properties of graphitic and non-graphitic carbons by Raman spectroscopy. *Carbon* **2020**, *161*, 359–372, doi:10.1016/j.carbon.2019.12.094.

7. Campbell, I.H.; Fauchet, P.M. The effects of microcrystal size and shape on the one phonon Raman spectra of crystalline semiconductors. *Solid State Communications* **1986**, *58*, 739–741, doi:10.1016/0038-1098(86)90513-2.

8. Fauchet, P.M.; Campbell, I.H. Raman spectroscopy of low-dimensional semiconductors. *Critical Reviews in Solid State and Materials Sciences* **1988**, *14*, s79-s101, doi:10.1080/10408438808244783.

9. Schüpfer, D.B.; Badaczewski, F.; Peilstöcker, J.; Guerra-Castro, J.M.; Shim, H.; Firoozabadi, S.; Beyer, A.; Volz, K.; Presser, V.; Heiliger, C.; et al. Monitoring the thermally induced transition from sp3-hybridized into sp2-hybridized carbons. *Carbon* **2021**, *172*, 214–227, doi:10.1016/j.carbon.2020.09.063.